

Disclaimer/Publisher's Note: The statements, opinions, and data contained in all publications are solely those of the individual author(s) and contributor(s) and not of MDPI and/or the editor(s). MDPI and/or the editor(s) disclaim responsibility for any injury to people or property resulting from any ideas, methods, instructions, or products referred to in the content.

Review

# Li-rich layered oxides: structure and doping strategies to enable Co-poor/Co-free cathodes for Li-ion batteries

Laura Silvestri <sup>1</sup>, Mariarosaria Tuccillo <sup>2</sup>, Arcangelo Celeste <sup>1,2</sup> and Sergio Brutti <sup>2,\*</sup>

<sup>1</sup> Dipartimento di Tecnologie Energetiche e Fonti Rinnovabili, ENEA C.R. Casaccia, via Anguillarese 301, Roma (Italy); [laura.silvestri@enea.it](mailto:laura.silvestri@enea.it)

<sup>2</sup> Dipartimento di Chimica, Sapienza Università di Roma, p.le Aldo Moro 5, Roma (Italy) [mariarosaria.tuccillo@uniroma1.it](mailto:mariarosaria.tuccillo@uniroma1.it), [arcangelo.celeste@uniroma1.it](mailto:arcangelo.celeste@uniroma1.it), [sergio.brutti@uniroma1.it](mailto:sergio.brutti@uniroma1.it)

\* Correspondence: [sergio.brutti@uniroma1.it](mailto:sergio.brutti@uniroma1.it)

**Abstract:** Lithium rich layered oxides (LRLO) are a wide class of innovative active materials for positive electrodes in lithium-ion (LIB) and lithium-metal secondary batteries (LMB). LRLOs are over-stoichiometric layered oxides rich in lithium and manganese, with general formula  $\text{Li}_{1+x}\text{TM}_1-x\text{O}_2$ , where TM is a blend of transition metals comprising Mn (main constituent), Ni, Co, Fe and others. Due to the very variable composition and the extended defectivity their structural identity is still debated among researchers being likely an unresolved hybrid between a monoclinic (mC24) and a hexagonal lattice (hR12). Once casted in composite positive electrode films and assembled in LIBs or LMBs, LRLOs can delivery reversible specific capacities above 220-240 mAhg<sup>-1</sup>, thus beyond any other available intercalation cathode material for LIBs, with mean working potential above 3.3-3.4 V vs Li for hundreds of cycles in liquid aprotic commercial electrodes. In this review we critically outline the recent advancements in the fundamental understanding of the physico-chemical properties of LRLO as well as the most exciting innovations in their battery performance. We focus in particular on the elusive structural identity of these phases, on the complexity of the reaction mechanism in batteries as well as on practical strategies to minimize or remove cobalt from the lattice while preserving the outstanding performance upon cycling.

**Keywords:** lithium rich layered oxides; secondary aprotic batteries; positive electrode materials; Li-ion; cathodes.

## 1. Introduction

Effective and sustainable energy storage is a key societal challenge for the enforcement of reliable collective actions at world level to mitigate the CO<sub>2</sub> concentration increase in the earth atmosphere and possibly to pave the way for its reduction in the second half of this century. [1] Currently a variety of technologically accessible energy storage devices are on the market, each tackling a specific need, thus filling a specific market niche. As an example, water dams deal with massive energy storage to supply power to the energy grids in the consumption peaks, lead-acid batteries are unavoidable power devices to start internal combustion engines in cars, whereas Li-ion batteries feed energy in all our innumerable electronic mobile apparatuses. [2] On the other hand, the market diffusion of electric vehicles as well as the upgrade to the national-wide energy grids to continental-based smart energy networks is pushing the current energy storage technologies to their limits, thus requiring innovative breakthrough.

Li-ion batteries (LIBs) are the most remarkable success case in the energy storage technology landscape in the last fifty years: [3] their unique configuration allow a fine tuning of performance and properties to meet diversified application needs thanks to the flexible combination of positive electrodes/electrolyte/negative electrodes components. [4,5] Since their market presentation in the early 90s, the most limiting performance factors of LIBs deal with costs and the gravimetric specific capacity limits. To tackle these

drawbacks, the international R&D community has been working hard in the last thirty years to shift from LiCoO<sub>2</sub> to high-capacity positive electrode materials, from carbonate-based liquid electrolytes to solid state ones, and from graphite to high-capacity negative electrode materials. [3,6] Recently the European Union categorized various battery chemistries in “generations” starting from the (+)LiCoO<sub>2</sub>/EC:DMC LiPF<sub>6</sub>/graphite(-) Generation 1 (i.e. EC=ethylene carbonate, DMC=dimethyl carbonate) to the innovative Generation 3a and 3b (high capacity lithium-ion batteries), Generation 4a (solid state lithium metal batteries), Generation 4b (lithium-sulphur batteries) and Generation 5 (lithium-oxygen and beyond-lithium batteries). [7] Currently battery manufacturers are addressing the transition from Generation 2 to Generations 3a and 3b whereas all next generations are still under development in R&D laboratories worldwide. It is important to underline that the most remarkable bottleneck of generation 3a and 3b is the capacity limitation of positive electrodes, that barely exceed 150 mAhg<sup>-1</sup> in respect to the mass of the cathode active material. Given this meagre gravimetric performance, it is not surprising that positive electrodes accounts for the majority of the sum of the active material mass (negative + positive sides) in any Li-ion battery (e.g. twice the mass of graphite, five times the mass of tin, twenty times the mass of silicon, being C, Sn and Si popular negative electrode materials for Li-ion batteries). Thus, any capacity improvement of positive electrode materials highly impacts the overall performance of the entire battery and motivates the strong driver in R&D to develop innovative families of cathode materials (e.g. Ni-rich layered oxides, high voltage phospho-olivines, fluoro-phosphates). [8–10] Among these, lithium rich layered oxides are playing a pivotal role in recent years thanks to their compositional flexibility, very high practical capacities exceeding 200–220 mAhg<sup>-1</sup>, satisfactory working potential (3.3–3.6 V vs Li), good environmental compatibility and manufacturing processes similar to those for standard layered oxides. [11,12]

Lithium-rich layered oxides (LRLO) are over-stoichiometric oxides rich in lithium and manganese, with general formula Li<sub>1+x</sub>TM<sub>1-x</sub>O<sub>2</sub>, where TM is a blend of transition metals comprising Mn (main constituent), Ni, Co, Fe and others. Once formulated in positive electrode composite films, these materials demonstrate in aprotic lithium-metal and in aprotic lithium-ion batteries excellent reversible performance for hundreds of charge/discharge cycles: their unique functional properties roots in the peculiar composition, structure, and extended disorder at crystalline level. The R&D efforts in this field is very intense to develop innovative materials with minor (or even absent) Co-content (cobalt is a critical raw material), able to deliver in battery high coulombic efficiencies and high-capacity retentions for thousands of cycles, that can be manufactured using facile and environmentally feasible protocols.

In this review we outline the recent advancements in the fundamental understanding of the physico-chemical properties of LRLO as well as the most exciting innovations in their battery performance. Here, we focus specifically on the analysis of the elusive LRLO crystal structure and de-lithiation/lithiation mechanism in Li-ion batteries as well as on the strategies to minimize or remove cobalt from the LRLO lattice without damaging the performance.

## 2. Structure and reaction mechanism

Li-rich layered oxide (LRLO) cathode materials show an ambiguous crystalline structure, still debated among researchers. The typical X-ray diffraction (XRD) pattern experimentally observed any LRLOs can be index with the  $\alpha$ -NaFeO<sub>2</sub>-type structure (see figures 1a and 1b), or O3-type. This prototypal structure consists of transition metals layers TMs-based edge-sharing TM-O<sub>6</sub> octahedral (TM=Ni, Co, Mn etc. in 3b site), separated by layers of Li<sup>+</sup> (3a site), where the oxygen planes (6c site) have an ABCABC stacking sequences, and adopt R $\bar{3}m$  symmetry (hR12). [13] However, XRD patterns of all LRLOs reported in the literature also show broad and weak peaks in the 20°–30° range (excitation wavelength, Cu K $\alpha$ ) that cannot be indexed by adopting the hR12 lattice. Currently these diffraction lines are considered a clue of the existence of an unresolved superstructure with Li<sub>2</sub>MnO<sub>3</sub>

symmetry crystallizing in a monoclinic layered structure that adopts a  $C2/m$  space group ( $mC24$ ), as reported in figure 1b. [14–16] In this lattice, Li ions occupy inter-slab octahedral sites (4h and 2c) and slab octahedral sites (2b and 4g) together with Mn ions in (1:2) ratio, whereas oxygen atoms occupies 4i and 8j sites. The layered structure of  $\text{Li}_2\text{MnO}_3$  is often described by using the notation  $\text{Li}[\text{Li}_{1/3}\text{Mn}_{2/3}]\text{O}_2$  where Mn ions are partially replaced by Li ions and  $\text{Li}^+$  and  $\text{Mn}^{4+}$  form a locally ordered honeycomb structure. [17,18]

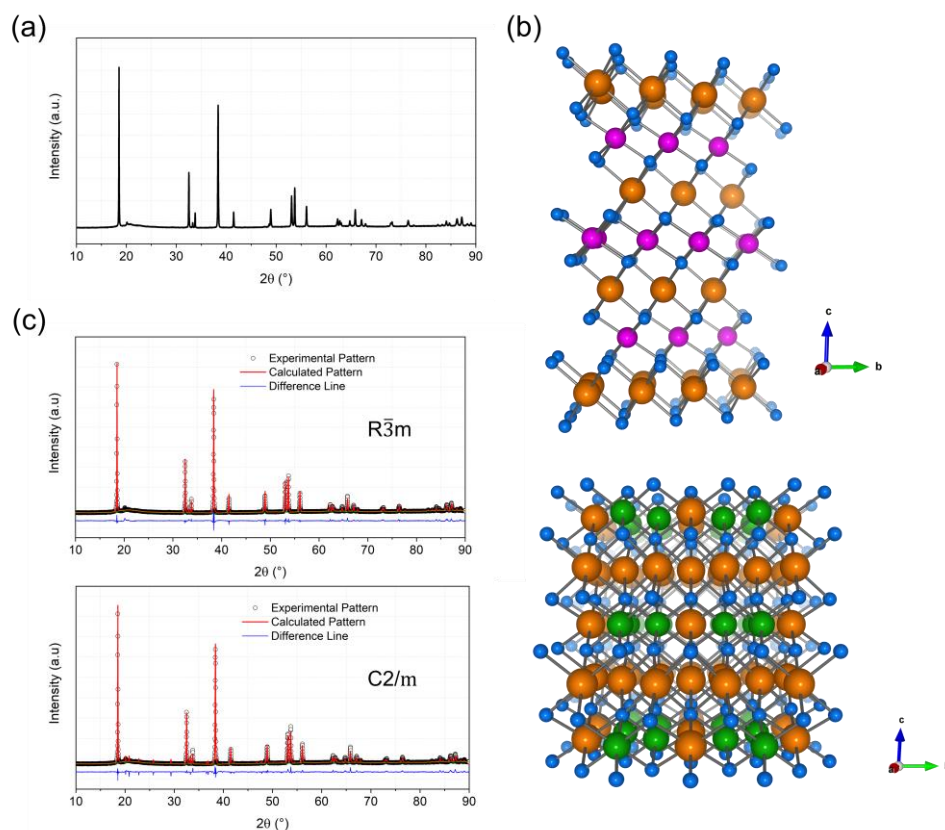


**Figure 1.** a) XRD pattern of  $\text{Li}_{1.2}\text{Mn}_{0.54}\text{Ni}_{0.13}\text{Co}_{0.13}\text{O}_2$  acquired with a Rigaku SmartLab (Bragg-Brentano geometry,  $\text{CuK}\alpha$  radiation), b) pictorial structure of  $\text{LiCoO}_2$  ( $R\bar{3}m$  symmetry) and  $\text{Li}_2\text{MnO}_3$  ( $C2/m$  symmetry) where Li and metals layers can be seen. Lithium is orange, Co is magenta, Mn is green, and O is blue, c) Rietveld refinement obtained with GSAS-II of XRD pattern assuming  $R\bar{3}m$  or the  $C2/m$  symmetry.

The above-mentioned superstructure peaks originate from the symmetry-allowed X-ray coherent scattering from lattice-planes, induced by the ordered  $\text{LiMn}_6$  motifs in the TMs layer. Thus, single phase Rietveld refinement unavoidably fails to fully achieve an accurate structural reconstruction either assuming the  $R\bar{3}m$  or the  $C2/m$  prototype structures (figure 1c), being the real structure a hybrid intermediate.

Due to these structural peculiarities, there is not a general consensus in the way LRLO lattice is analyzed and discussed in the literature. In most cases LRLOs have been described by using one between two very popular notations [19]:

- (a)  $(1-x)\text{Li}_2\text{MnO}_3 \cdot x\text{LiMO}_2$ , as nano-composite of  $R\bar{3}m$  and  $C2/m$ ;
- (b)  $\text{Li}_{1+x}\text{M}_{1-x}\text{O}_2$ , as a single solid solution.

According to Thackeray et al. [20] the structure of LRLOs have a composite character consisting of nanometer regions with  $\text{Li}_2\text{MnO}_3$ - and  $\text{LiTMO}_2$ -like features. Bareño et al. [21] through a combination of diffraction, microscopy and spectroscopy proposed a dendritic microstructure, where  $\text{LiCoO}_2$ - and  $\text{Li}_2\text{MnO}_4$ -like structures coexists. The study on  $\text{Li}[\text{Li}_{0.2}\text{Mn}_{0.6}\text{Ni}_{0.2}]\text{O}_2$  reported by Gu et al. [22] suggested a nanoscale composite with a structural integration of  $\text{LiMO}_2$   $R\bar{3}m$  phase with  $\text{Li}_2\text{MnO}_3$   $C2/m$  phase. In particular, by the use of atomic-scale Z-contrast imaging, x-ray energy-dispersive spectroscopy (XEDS)

and electron energy loss spectroscopy (EELS), they observed the Ni segregation at the surface layers and grain boundaries, with concentration increases gradually from <20% in the inner part of particle to 50% in some superficial regions, while Mn is abundant in the core and deficient in the surface region. Despite oxygen had a more uniform distribution, it was observed an increasing of oxygen concentration in the inner part of particles. Furthermore, Aurbach et al. [23,24] investigated a nanoscale composite structure of  $0.5\text{Li}_2\text{MnO}_3\text{-}0.5\text{LiMn}_{1/3}\text{Ni}_{1/3}\text{Co}_{1/3}\text{O}_2$  demonstrating that the rhombohedral  $\text{LiNiO}_2$ -like and monoclinic  $\text{Li}_2\text{MnO}_3$  structures are integrated and interconnected at the atomic level.

On the contrary, Jarvis et al. [14,22] reported the  $\text{Li}[\text{Li}_{0.2}\text{Mn}_{0.6}\text{Ni}_{0.2}]\text{O}_2$  as a single-phase solid solution with long range lithium ordering resulting in a  $C2/m$  symmetry since they had no evidence of two-phase behavior. The studies conducted by Lu et al. [25] confirmed that these compounds are true solid solutions of  $\text{Li}_2\text{MnO}_3$ -like structure. Also Koga et al. [26] affirmed that  $\text{Li}_{1.2}\text{Mn}_{0.54}\text{Co}_{0.13}\text{Ni}_{0.13}\text{O}_2$  has a rhombohedral  $R\bar{3}m$  structure with long-range  $\sqrt{3}a_{\text{hex}} \times \sqrt{3}b_{\text{hex}}$  cation ordering using ND and electron diffraction associated with NMR and Raman spectroscopy. The electron diffraction pattern observed along the  $[1\text{-}10]$  zone axis cannot be considered as a simple combination or nanocomposite of typical  $\text{Li}_2\text{MnO}_3$  and  $\text{LiMO}_2$  materials. These results are in good agreement with the work of Jarvis et al. [27], that reported a monoclinic structure with a significant number of thin planar defect along (001) planes based on diffraction STEM (D-STEM). Ates et al. [28] confirmed the presence of a single  $C2/m$  solid solution using selected area electron diffraction (SAED), because some of the diffraction patterns can be solely indexed to this phase.

Overall, the large compositional variety of LRLOs and their high defectivity even increase its structural complexity thus making any facile structure clarification ambiguous and incomplete. In fact, several groups demonstrated the presence of multiple thin planar defects along the transition metal layers and report these defects as stacking faults [21,29–31] or as defect-point, anti-site defect. [16,32,33] Moreover, structural properties vary with the composition and with the synthetic technique used, from precursor mixing and annealing conditions. [34–37]

The structural ambiguity of LRLOs directly reflex on to the sluggish rationalization of the corresponding redox mechanism in batteries and the unsatisfactory comprehension of the structural evolution occurring during repeated cycles of electrochemical lithium-ions extraction/insertion. In the figure 2a the typical potential profile of the first cycle obtained is shown for a LRLO with the  $\text{Li}_{1.2}\text{Mn}_{0.54}\text{Ni}_{0.13}\text{Co}_{0.13}\text{O}_2$  stoichiometry. [38] The first electrochemical process shows a two steps charge profile: a slope up to 4.4V where the Li extraction is balanced from the oxidation of transition metals ( $\text{Co}^{3+}/\text{Co}^{4+}$  and  $\text{Ni}^{2+}/\text{Ni}^{3+}/\text{Ni}^{4+}$ ) and a long plateau above 4.5V where the further lithium removal is balanced by the activation of  $\text{O}^{2-}/\text{O}$  redox couple. [39–42] The manganese is not involved in this first electrochemical process due to its stability in +4 oxidation state. The potential profile changes drastically after the first charge (figure 2b), as well as in the following cycles, leading to the so-called voltage (or working potential) decay upon cycling and the increase of the voltage hysteresis between charge and discharge.

Focusing on the first cycle, it is important to underline that, the electrochemical reaction occurring along the 4.5 V vs Li plateau in the first cycle is only partially reversible and disappears during the discharge step. In fact, the reinsertion of  $\text{Li}^+$  in the LRLO occurs not only exploiting the Co/Ni/O redox couples but also by the reduction of  $\text{Mn}^{4+}$  to  $\text{Mn}^{3+/2+}$  near 2V. [39,43,44] The occurrence of lattice oxygen redox has been proposed in the literature to explain the extra capacity of LRLOs well beyond that achievable by exploiting the Ni/Co redox couples [41], and the observation of the  $\text{O}_2$  release in the first charge high voltage plateau. [45,46] However, the products of this anionic redox reaction are still object of discussion. Tarascon's group [47,48] proved the existence of O-O dimers and the formation of reversible  $\text{O}^{2n-}$  by XPS measurements on  $\text{Li}_2\text{Ru}_{1-y}\text{Mn}_y\text{O}_3$  and  $\text{Li}_2\text{Ru}_{0.75}\text{Sn}_{0.25}\text{O}_2$  compounds. Then, Li et al. [49] obtained the direct observation of O<sup>-</sup>-O<sup>-</sup> dimers bonding, mostly along the *c*-axis of  $\text{Li}_{1.2}\text{Ni}_{0.2}\text{Mn}_{0.6}\text{O}_2$ . Chen et al. [50] confirmed the formation of oxygen dimerization and the presence of molecular  $\text{O}_2$  in  $\text{Li}_2\text{MnO}_3$  using ab initio techniques. On the other hand, many authors proved that the oxygen redox evolves through oxygen

with holes,  $O^{n-}$  ( $n < 2$ ), rather than dimer species. Luo et al. [51,52] synthesized  $Li_{1.2}Mn_{0.54}Ni_{0.13}Co_{0.13}O_2$  and  $Li_{1.2}Mn_{0.6}Ni_{0.2}O_2$  and, in both materials, they demonstrated that  $Li^+$  removal is charge compensated by the formation of localized electron holes on O atoms coordinated by  $Mn^{4+}$  and  $Li^+$  ions. Gent et al. [53] proposed a novel mechanism in which the oxygen redox with the formation of holes is always coupled with transition metals migration,  $\{O^{2-} + TM\} \rightarrow \{O^- + TM_{mig}\} + e^-$ .

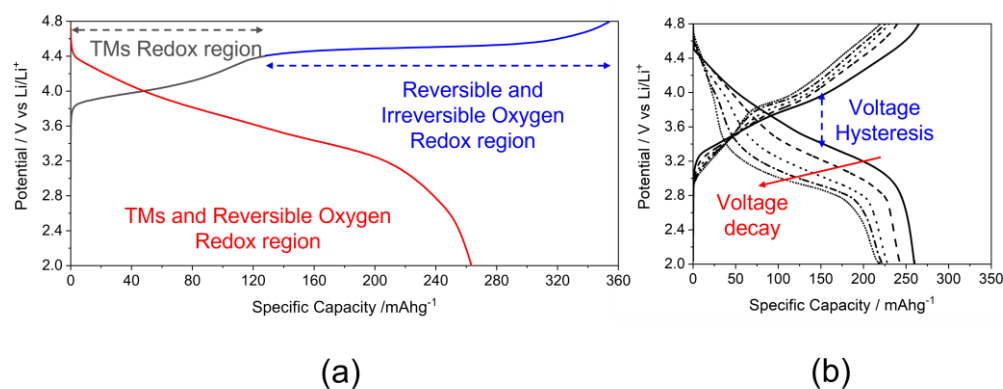


**Figure 2.** Typical potential profile of LRLOs a) upon first cycle and b) during prolonged cycling.

A direct effect induced by the molecular oxygen release in the phase composition and the structure of LRLOs after the first charge is the interdiffusion of metal cations from the bulk to the surface of the single crystal particles, and the consequent phase reorganization (figure 3). [54,55]

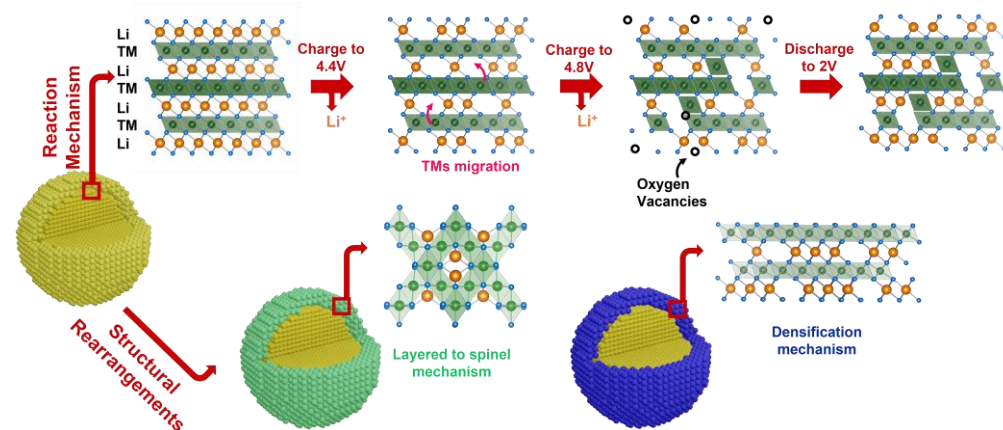


**Figure 3.** Schematic representation of the reaction mechanism of LRLOs during electrochemical Li de-intercalation/intercalation and resulting structural changes.

In fact, the oxygen redox activity has different structural effects in the particle bulk and on their surface. When it occurs in the bulk, it is reversible and increase the specific capacity delivered by LRLOs as demonstrated by Assat et al. with the use of HAXPES technique. [56] While, when the redox activity occurs in proximity to the particle surface, it facilitates the irreversible release of molecular oxygen leaving 0D vacancies in the LRLO anionic sublattice. [57] As a consequence, and unavoidably, the accumulation of oxygen vacancies promotes cation mixing, stacking faults, segregation of new phases and irreversible change in the oxidation state of metals. This structural degradation mechanism has been analyzed in detail by Cui et al. that, supported by XRD, HRTEM and SAED measurement [58], proposed a multi-step process. The structural degradation of LRLOs consists of an initial stage associated to the irreversible loss of part of lattice oxygen and

formation of oxygen vacancies on the surface followed by the migration of transition metal ions into the lithium layer. This interdiffusion results in a further cation mixing and triggers a layered to spinel structure transformation. The evidence of the formation of a new spinel-like solid phase on the surface of electrodes after the first charge has been proved also by other groups. Xu et al. [59] investigated the surface changes of the samples before and after electrochemical cycling through Electron Energy Loss Spectroscopy (EELS) measurements whereas Boulineau et al. [60] reported the first evidence of Mn-Ni segregation, highlighting the motion of Mn ions from the surface to bulk, while spinel distortion occurs on the surface, with thickness of about 2-3 nm. Other groups described the phase evolution of LRLOs upon cycling with the occurrence of a material densification and phase degradation as reported by Armstrong et al. in 2006. [46] Under this hypothesis the oxygen release leaves oxygen vacancies near the surface with consequent migration of TM ions from the surface to the bulk to occupy the empty Li octahedral sites in TM layers. This ion diffusion further induces the segregation along the radius of a single crystal particle of an inner core and outer layer, each with a different composition and density. Delmas and co-workers [61,62] extensively studied the structural evolution of LRLOs. They confirmed the densification model with ex-situ X-Ray diffraction during the first cycle. The densified phase grows from the surface while the inner of the particles does not change. Recently, Celeste et al. [63,64] extended the analysis beyond the first cycle on  $\text{Li}_{1.2}\text{Mn}_{0.54}\text{Ni}_{0.13}\text{Co}_{0.13}\text{O}_2$  and  $\text{Li}_{1.28}\text{Mn}_{0.54}\text{Ni}_{0.13}\text{Co}_{0.02}\text{Al}_{0.03}\text{O}_2$  using XRD and Raman Spectroscopy. From the XRD analysis, the patterns showed the formation of a new phase during the first charge with a very similar structure to the pristine one. Apparently both pristine and densified phases can further reversibly exchange lithium ions cycle-by-cycle, while their relative amount changes. Remarkably Celeste et al. proved by Raman spectroscopy the appearance of a peak shoulder possibly attributed to the spinel-distortion, thus suggesting even more complex multiphase mechanisms from the inner core to outer layers of the primary particles of LRLOs. [63,64]

### 3. Open challenges for the development of LRLOs

The full comprehension of the structural complexity of LRLOs and of their detailed reaction mechanism are essential elements to make these materials suitable for the commercialization. As discussed in the previous section, the current consensus is that the extra-capacity delivered by LRLOs beyond the tetravalent oxidation state of transition metal ions is due to the anion redox reaction. However, the exact nature and identity of the products of this oxygen redox reaction (e.g. superoxidic or peroxidic pairs, de-localized distributed negative charge loss in the anionic sublattice, localized charged vacancies in the lattice, either cationic or anionic) is difficult to reveal and quantify, and is likely interplayed with the long term cycling behavior of any LRLOs. [41,42,46,48,54,61,62,65–69] It is likely that the redox mechanisms involving the oxygen redox couples is related to the local and mean composition of the LRLO, being the nature of the oxidized species closely dependent on the covalency of metal-oxygen bond [49,52,53,70], the presence of cationic vacancies near the oxygen, the activation of migrations, the existence of charged vacancies in the negative sublattice, the lithium concentration in the TM layer etc. Furthermore, and unavoidably, also any  $\text{O}_2$  release in the first charge plateau [42,45,71,72] is necessarily interplayed with the formation of oxygen vacancies in the structure, the cation mixing, the formation of stacking faults, the segregation of a densified new phases and/or the irreversible changes in the oxidation state of metals. [58,60,73,74] Remarkably, it is not still clear if these vacancies, or other 0D defects, are either a bulk or a surface phenomenon and if they can migrate from the surface to the bulk or vice-versa. Overall, the redox crystal chemistry and phase phenomena occurring in the electrochemical de-lithiation/lithiation of any LRLO is a very intricate process and, surely, affects the cycling performances and origins the potential fading upon cycling.

From the structural point of view, the main consequences of the exploitation of the anionic redox activity are a gradual coordination transformation around the TMs and in

the layer stacking. The exact degradation mechanisms are not fully understood and many hypotheses have been discussed and validated on specific LRLO compositions ranging from a structural shift to form a spinel structure [75,76] to the formation of densified layers. [54,62,77] Furthermore, the oxygen loss from the lattice is also interplayed with side reactions with non-aqueous electrolytes during the first de-lithiation leading to the formation of lithium oxide, lithium carbonate, organic species, and the release of protons in the electrolytes. [46,65] These undesired electrochemical processes likely contribute to the large irreversible capacity loss and the low Coulombic efficiency observed in the first cycle.

Overall, the development of effective and reliable LRLOs is challenged by a varied of drawbacks that is important to rationalize and understand to improve the initial Coulombic efficiency, mitigate the working potential decay upon cycling and increase the rate performance. Nonetheless, the foreseen competitiveness of these materials in the battery market is challenged by the need of optimized manufacturing procedures to reduce costs using sustainable raw-materials supplies, and to integrate their production into already existing industrial protocols and infrastructures. In this respect, the removal of cobalt from the structure of LRLOs is a key-issue to improve their environmental compatibility, minimize the need of critical raw materials in the manufacture and reduce the costs. [78,79] Cobalt substitution can be achieved by a balanced blend of other metals. However, any alteration of the metal blend in the transition metal layer has inevitable effects on the electronic and crystallographic structure of the LRLOs as well as on its thermodynamic stability, thus affecting the resulting battery performance. Computational studies suggests that the reduction in the Co content in the LRLO lattice leads to an expansion of the structures due to the greater electronic distortions, i.e. Jahn-Teller defects. [80,81] This structural effect can promote the mobility of lithium ions thanks to the weaker coordination but also promotes the cation interdiffusion and reduces the electronic density of states at the Fermi level, possibly negatively impacting the electronic conductivity. [81]

#### 4. Progresses on doping strategies for LRLOs

Doping is one of the most used strategies to improve the structural stability, mitigate the voltage fading and reduce the capacity loss of LRLOs. This strategy has been adopted also to reduce, or completely remove, cobalt from the structure. In this paragraph, we summarize current advancements to outline a comprehensive overview about the use of doping to obtain Co-poor or Co-free LRLOs.

##### 4.1. Co-poor LRLOs

Cobalt substitution is a remarkable challenge that unbalance the electronic structure and alters the thermodynamic stability of LRLOs. An example Kou et al. [82] showed the negative effect of the reduction of cobalt content on the discharge capacities and working voltages of a homologous series of LRLOs with general formula  $\text{Li}_{1.2}\text{Ni}_{0.2-x}\text{Co}_{2x}\text{Mn}_{0.6-x}\text{O}_2$  ( $x=0-0.05$ ). In recent years, many different doping strategy or compositions have been investigated to prove the feasibility of Co-free or Co-poor LRLO with promising performance in LIBs.

One of the most studied stoichiometry of LRLOs is  $\text{Li}_{1.2}\text{Mn}_{0.54}\text{Ni}_{0.13}\text{Co}_{0.13}\text{O}_2$  and it is often used as a benchmark point for understanding the impact of the reduction of cobalt by changing the Ni:Co:Mn ratio or by introducing new elements. Ramesha et al. [83] prepared a series of LRLOs materials by varying the Ni, Mn and Co contents to identify the optimal ratio. In particular,  $\text{Li}_{1.2}\text{Ni}_{0.32}\text{Co}_{0.04}\text{Mn}_{0.44}\text{O}_2$  shows very small voltage decay and a capacity retention of 85% after 100 cycles. Redel et al. [84] investigated various stoichiometries,  $\text{Li}[\text{Li}_y\text{Mn}_{1-y-2z}\text{Ni}_z\text{Co}_z]\text{O}_2$ , aiming at the reduction of cobalt: the stoichiometry  $\text{Li}[\text{Li}_{0.2}\text{Mn}_{0.6}\text{Ni}_{0.1}\text{Co}_{0.1}]\text{O}_2$  showed the best compromise between Co amount and electrochemical properties. In fact, the specific capacities and lithium diffusion coefficients decrease too much when cobalt is less than 0.1 in the structure. Hamad et al. [85] studied the interplay of cobalt and nickel contents in the LRLO by systematically study an homologue

series of materials with stoichiometry  $\text{Li}_{1.2}\text{Mn}_{0.51}\text{Ni}_{0.145+x}\text{Co}_{0.145-x}\text{O}_2$  ( $x = 0, 0.0725$ ). Despite the initial drop in the specific capacity, the Co-poor sample has an activated trend in the first charge/discharge cycles with better capacity retention at the end of test compared to the Co-rich. The superior performance in  $\text{Li}_{1.2}\text{Mn}_{0.51}\text{Ni}_{0.0725}\text{Co}_{0.0725}\text{O}_2$  was attributed to the continuous activation of the  $\text{Li}_2\text{MnO}_3$  lattice.

Besides altering the Co:Mn:Ni relative ratios, the cobalt reduction can be achieved by isovalent or aliovalent doping with other cations. As an example, Bao et al. [86] proposed a series of Yb doped lithium rich materials,  $\text{Li}_{1.2}\text{Ni}_{0.13}\text{Co}_{0.13-x}\text{Yb}_x\text{Mn}_{0.54}\text{O}_2$ . The best materials obtained, with  $x=0.005$ , exhibited a discharge capacity of 250.3 and 219.8  $\text{mAhg}^{-1}$  at 0.2 and 1C, respectively. Capacity retentions were 87.3 and 84.4% after 50 cycles at 0.2 C and 100 cycles at 1C. Kou et al. [87] prepared a series of Ti doped Co-poor Lithium Rich,  $\text{Li}_{1.167}\text{Ni}_{0.4-x}\text{Mn}_{0.383}\text{Co}_{0.05}\text{Ti}_x\text{O}_2$  ( $x = 0, 0.02, 0.04$  and  $0.08$ ). Ti doping have an impact on electrochemical performance and the doped material with  $x=0.04$  showed the best performances. It has a discharge capacity of 187  $\text{mAhg}^{-1}$  with a capacity retention of 99.4% after 10 cycles at 0.1 C.

Among others, aluminium doping has been extensively used by many authors. Guo et al. [88] proposed an Al-doped material with formula  $\text{Li}_{1.14}(\text{Ni}_{0.136}\text{Co}_{0.10}\text{Al}_{0.03}\text{Mn}_{0.544})\text{O}_2$  in close comparison with the Co-rich  $\text{Li}_{1.14}(\text{Ni}_{0.136}\text{Co}_{0.136}\text{Mn}_{0.544})\text{O}_2$ . The doped samples showed a slight decrease in discharge capacity but also improved cycling stability due to the apparent stabilization of the overall structure. Thang et al. [89] used Sol-Gel process to synthesize  $\text{Li}[\text{Li}_{0.2}\text{Ni}_{0.15}\text{Mn}_{0.55}\text{Co}_{0.1-x}\text{Al}_x]\text{O}_2$  ( $x = 0, 0.025, 0.05, 0.075$ ) and found that the optimum doping content of Al is about 0.05. In fact, the  $\text{Li}_{1.2}\text{Ni}_{0.15}\text{Mn}_{0.55}\text{Co}_{0.05}\text{Al}_{0.05}\text{O}_2$  stoichiometry can achieve 237  $\text{mAhg}^{-1}$  and showed an improved structural stability. Also, niobium has been studied as a doping element thanks to the ability to mitigate the discharge voltage decay, decrease the charge-transfer resistance, and improve the lithium ion diffusion coefficient. [90,91] Dong et al. [90] used solvothermal method to prepare a homologue series of LRLOs with general stoichiometry  $\text{Li}_{1.2}(\text{Ni}_{0.13}\text{Co}_{0.13}\text{Mn}_{0.54})_{1-x}\text{Nb}_x\text{O}_2$ , where  $x = 0, 0.01, 0.02, 0.04$ . Samples with Nb amount equal to 0.02 can achieve a specific capacity of 271  $\text{mAhg}^{-1}$  and a capacity retention of 98% after 300 cycles. Dong et al. also proved that Nb can effectively stabilizes the crystal structure and improve the charge transfer resistance upon cycling. Recently, Liu et al. [91] confirmed the beneficial effects of Nb traces in Co-poor LRLOs by demonstrating an optimized LRLO stoichiometry, namely  $\text{Li}_{1.14}\text{Mn}_{0.466}\text{Ni}_{0.249}\text{Co}_{0.046}\text{Al}_{0.015}\text{Nb}_{0.02}\text{O}_2$ . This material apparently exhibited excellent electrochemical performance as Nb doping improved the first cycle reversibility leading to a remarkable capacity retention of 93% after 200 cycles.

Iron is earth-abundant element and is one of the best choices to replace cobalt thanks to its limited cost and the +3 stable oxidation state, like aluminum ions: in fact, many author proved that iron can be used to stabilize the electrochemical behavior of LRLOs. Nayak et al. [92] used iron to partly replace cobalt, obtaining a material with formula  $\text{Li}_{1.2}\text{Mn}_{0.56}\text{Ni}_{0.16}\text{Co}_{0.04}\text{Fe}_{0.04}\text{O}_2$ . The doped material can deliver a specific capacity of 254  $\text{mAhg}^{-1}$  and showed better rate capability and better structural stability than the Co-rich benchmark. More recently, Yi et al. [93] synthesized a series of materials with general stoichiometry  $\text{Li}_{1.2}\text{Mn}_{0.56}\text{Ni}_{0.16}\text{Co}_{0.08-x}\text{Fe}_x\text{O}_2$  ( $x = 0, 0.01, 0.03, 0.05, 0.08$ ), and observed that the reversible capacity of the doped samples is larger compared to the undoped benchmark at very high current density. In particular, the sample  $x=0.05$ ,  $\text{Li}_{1.2}\text{Mn}_{0.56}\text{Ni}_{0.16}\text{Co}_{0.03}\text{Fe}_{0.05}\text{O}_2$ , showed the best performance with minor charge transfer resistance and enhanced Li-ion diffusion. Medvedeva et al. [94] prepared an iron doped material, i.e.  $\text{Li}_{1.2}\text{Ni}_{0.133}\text{Mn}_{0.534}\text{Co}_{0.118}\text{Fe}_{0.016}\text{O}_2$ , able to deliver excellent capacity retention thus confirming the strong mitigation of the voltage decay induced by the incorporation of the isovalent iron as dopant. After 100 charge/discharge cycles, the discharge voltage potentials are 3.3V and 3 V, for doped and undoped samples respectively, indicating the beneficial effect of iron to improve the structural resilience of LRLO upon cycling.

On the other hand, Nisar et al. [95] successfully synthesized various Cr-doped lithium-rich phases, i.e.  $\text{Li}_{1.2}\text{Ni}_{0.16}\text{Mn}_{0.56}\text{Co}_{0.08-x}\text{Cr}_x\text{O}_2$  (where  $x = 0.00, 0.01$ , and  $0.02$ ), by the sol-gel method. Apparently, the chromium doping stabilizes the electrochemical performance

in prolonged galvanostatic test as well as the interface stability between material and electrolyte.

Co-doping has also been used in recent years to exploit synergistic effects arising from the simultaneous presence of two dopants. Ghorbanzadeh et al. [96] proposed Al/Zr co-doping in LRLO, i.e.  $\text{Li}[\text{Li}_{0.2}\text{Ni}_{0.13-x+y/3}\text{Co}_{0.13-x+y/3}\text{Mn}_{0.54-x+y/3}]\text{Al}_x\text{Zr}_y\text{O}_2$  ( $x = 0, 0.02, 0.03$  and  $y = 0, 0.015, 0.03$ ). They demonstrated that the presence of Al improves the structural stability while the Zr enhances the specific capacity and the lithium diffusion. Celeste et al. [63,97] focused on the substitution of cobalt with lithium (over-lithiation) and aluminium, leading to a family of materials with general formula  $\text{Li}_{1.2+x}\text{Mn}_{0.54}\text{Ni}_{0.13}\text{Co}_{0.13-x-y}\text{Al}_y\text{O}_2$ , where  $0.03 \leq x \leq 0.08$  and  $0.03 \leq y \leq 0.05$ . Apparently, the decrease of the cobalt content leads to an expansion of the unit cell, due to the huge difference in the ionic radius of  $\text{Co}^{3+}$  and  $\text{Li}^+$ . Moreover, relevant changes have been seen in the electrochemical behaviour. The potential profiles during the first cycle highlights a alteration of the two-stage redox reaction in the first charge (slope below 4.4 V followed by the long pseudo-plateau at 4.5 V vs Li). Overall, the capacity delivered from the oxidation of transition metals decreases due to the redox inactivity of lithium and aluminium, while the increase of the ionicity of the metal-oxygen bonds partially decrease the extent of the high voltage plateau. This combination of effects leads to a net increase of the first cycle coulombic efficiency. Furthermore, despite the reduction of the overall delivered capacity, all samples can reversibly exchange specific capacities over  $200 \text{ mAhg}^{-1}$ , showing outstanding cycling stability.

The impact of a pseudo n-doping on the LRLO crystal and electronic structures has been elucidated by comparing the performance and properties of  $\text{Li}_{1.28}\text{Mn}_{0.54}\text{Ni}_{0.13}\text{Co}_{0.02}\text{Al}_{0.03}\text{O}_2$  in close comparison with a Co-rich material, namely  $\text{Li}_{1.2}\text{Mn}_{0.54}\text{Ni}_{0.13}\text{Co}_{0.13}\text{O}_2$ . [97] The replacement of Co with Al and Li leads to the occurrence of native oxygen vacancies and changes in the electronic structure. In fact, XANES measurements demonstrated an increase in the net oxidation state of the nickel centers with the formation of a small amount of  $\text{Ni}^{3+}$  and an increase in the Jahn–Teller defects compared to the Co-rich sample. The most relevant beneficial effect of this strategy is the remarkable reduction of the voltage decay: this behavior can be correlated to the improvement in the LRLO structure stability upon cycling, in fact, postmortem XRD patterns and Raman spectra showed the superior structural retention of  $\text{Li}_{1.28}\text{Mn}_{0.54}\text{Ni}_{0.13}\text{Co}_{0.02}\text{Al}_{0.03}\text{O}_2$  compared to  $\text{Li}_{1.2}\text{Mn}_{0.54}\text{Ni}_{0.13}\text{Co}_{0.13}\text{O}_2$ . Feng et al. [98] used Ti and Zr co-doping to hinder oxygen losses during the first charge: the optimized material has an initial Coulombic efficiency of 84.2% and a suppressed voltage decay. Furthermore the specific capacity is  $229 \text{ mAhg}^{-1}$  with a capacity retention of 84% over 400 cycles.

Also anionic doping has been considered and demonstrated to stabilize Co-poor LRLOs. Zhang et al. [99] used  $\text{PO}_4^{3-}$  polyanions doping in  $\text{Li}(\text{Li}_{0.17}\text{Ni}_{0.20}\text{Co}_{0.05}\text{Mn}_{0.58})\text{O}_2$  to partly replace oxygen. In particular,  $\text{Li}(\text{Li}_{0.17}\text{Ni}_{0.20}\text{Co}_{0.05}\text{Mn}_{0.58})\text{O}_{1.95}(\text{PO}_4^{3-})_{0.05}$  showed improvements in stability and in the discharge midpoint potential. Also  $\text{SiO}_4^{4-}$  and  $\text{SO}_4^{2-}$  polyanions with a large radius have been introduced into LRLOs by Zhang et al [100] showing larger Coulombic efficiencies in the first cycle and enhanced energy retention upon cycling, as confirmed by the minor voltage decay in 400 cycles. In fact, after 400 cycles, the discharge capacities of  $\text{Li}(\text{Li}_{0.17}\text{Ni}_{0.20}\text{Co}_{0.05}\text{Mn}_{0.58})\text{O}_{1.95}(\text{SiO}_4)_{0.05}$  and  $\text{Li}(\text{Li}_{0.17}\text{Ni}_{0.20}\text{Co}_{0.05}\text{Mn}_{0.58})\text{O}_{1.97}(\text{SO}_4)_{0.03}$  sample are at  $200.4$  and  $215.4 \text{ mAhg}^{-1}$ , respectively, approximately 30% larger compared to  $\text{Li}(\text{Li}_{0.17}\text{Ni}_{0.20}\text{Co}_{0.05}\text{Mn}_{0.58})\text{O}_2$  ( $159.9 \text{ mAhg}^{-1}$ ).

#### 4.2 Co-free LRLOs

Among all the possible Co-free LRLO stoichiometries,  $\text{Li}_{1.2}\text{Mn}_{0.6}\text{Ni}_{0.2}\text{O}_2$  [101] is the most studied one. Amine et al.[69] proved that this material can exchange  $240 \text{ mAhg}^{-1}$  with anodic potential cutoff as high as 4.6V vs Li, but with limited reversibility since specific capacity of the first discharge is only of  $155 \text{ mAhg}^{-1}$ . However, the reversible specific capacity showed an activated trend being the discharge capacity at cycle 10 as large as  $205 \text{ mAhg}^{-1}$ . More recently, Manthiram et al. [102] demonstrated how the synthesis conditions

and calcination temperatures/duration can enhance the electrochemical performance of  $\text{Li}_{1.2}\text{Mn}_{0.6}\text{Ni}_{0.2}\text{O}_2$ .

Turning to other Co-free stoichiometries, Prakasha et al. [103] investigated the effect of the calcination temperature on the structural properties and the electrochemical performance of an LRLO with composition  $\text{Li}_{1.1}\text{Ni}_{0.35}\text{Mn}_{0.55}\text{O}_2$ . This material was synthesized by the use of spray-pyrolysis combined with a calcination at  $900^\circ\text{C}$ . Once casted in composite electrodes, this active material was able to deliver capacities of 180 and 100  $\text{mAhg}^{-1}$  at current rates of C/10 and 1C. A rationalization of the impact of the annealing temperature on transport properties was proposed by Tuccillo et al. using DFT and partially-disordered supercells: apparently the formation of large concentration of Ni/Li antisite defects between TM and Li layers can easily occur at temperatures larger than  $700^\circ\text{C}$ . [16]

Also in the case of Co-free LRLOs, isovalent and aliovalent metal doping (including  $\text{Na}^+$ ,  $\text{Nd}^{3+}$ ,  $\text{Al}^{3+}$ ,  $\text{Fe}^{3+}$ ,  $\text{F}^-$ ,  $\text{S}^{2-}$ ,  $\text{SO}_4^{2-}$  and  $\text{PO}_4^{3-}$ ) [104–110] was used as effective strategy to improve structural stability and decrease voltage decay upon long-term cycling. For instance, Manthiram et al. [109,110] reported a systematic study on the influence of cationic substitution on the reversible capacity of the first cycle. Manthiram suggested the possible inhibition of oxygen redox reaction by a tailored doping of the LRLO lattice. Specifically, they considered the substitution of Mn in  $\text{Li}_{1.2}\text{Mn}_{0.6-x}\text{Ni}_{0.2}\text{M}_x\text{O}_2$  with Ti and Mg and the substitution of Mn/Ni in equal amount in  $\text{Li}_{1.2}\text{Mn}_{0.6-0.5x}\text{Ni}_{0.2-0.5x}\text{M}_x\text{O}_2$  with Fe, Al, Cr and Ga. Using this strategy Manthiram demonstrated that the oxygen redox reaction and the extent of the first cycle high voltage plateau both decrease by increasing the covalency of metal-oxygen bonds in the lattice.

Laisa et al. [111] proved the enhancement of the functional properties in batteries of the parent  $\text{Li}_{1.2}\text{Mn}_{0.54}\text{Ni}_{0.13}\text{Co}_{0.13}\text{O}_2$  materials by complete substitution of  $\text{Co}^{3+}$  with  $\text{Fe}^{3+}$ . Both the Co- and Fe- LRLO showed capacity exceeding  $300 \text{mAhg}^{-1}$  in the first lithium de-insertion, but the reversibility of the Fe- LRLO was apparently doubled. In the same way, Wu et al. [112] used different contents of iron in a series of LRLOs with general formula  $\text{Li}_{1.2}\text{Mn}_{0.6-x/2}\text{Ni}_{0.2-x/2}\text{Fe}_x\text{O}_2$  ( $x = 0, 0.01, 0.03, 0.05$ ) to prove that that the capacity decrease occurring while removing cobalt can be compensated by an optimized iron content obtaining and excellent the first discharge capacity ( $\sim 232 \text{mAhg}^{-1}$ ) and reduced potential fading upon cycling, thanks to the suppression of Ni-ion migration from the TM layer to the Li one. Wei et al. [113] determined, using computational and experimental techniques, that the presence of  $\text{Fe}^{3+}$  in the LRLO lattice contributes to stabilize oxidized oxygen species in particular by avoiding the accumulation of dimers, thus enhancing the structural stability of the de-lithiated LRLO. Recently, Pham et al. [114] by combining operando OEMS (online mass spectrometry) and EIS (electrochemical impedance spectroscopy) experiments, proved the gas evolution of  $\text{CO}_2$ ,  $\text{O}_2$  and  $\text{POF}_3$  upon the first charge and matched the gaseous release with interface resistance modification at the cathode-electrolyte interface for an iron-doped LRLO with formula  $\text{Li}_{1.16}\text{Ni}_{0.19}\text{Fe}_{0.18}\text{Mn}_{0.46}\text{O}_2$ . Their study showed that the mitigation of oxygen evolution reaction can decrease the layered-to-spinel transition on the surface of the active material primary particles, thus leading to improved electrochemical performance upon cycling in half-cells.

Chromium doping was investigated by Dahn et al. [25,115] that systematically analyzed a series of LRLO with general formula  $\text{Li}[\text{Cr}_x\text{Li}_{(1/3-x/3)}\text{Mn}_{(2/3-2x/3)}]\text{O}_2$  (where  $x = 0, 1/6, 1/4, 1/3, 1/2, 2/3, 5/6, \text{ and } 1$ ). Apparently, by a fine tuning of the chromium content, it is possible to stabilize a reversible specific capacity of  $230 \text{mAhg}^{-1}$  with a mitigated loss of molecular oxygen. On the other hand Lee et al. [116] focused on the evaluation of the effect of Cr substitution on the voltage decay of the  $\text{Li}_{1.2}\text{Ni}_{0.2-x/2}\text{Mn}_{0.6-x/2}\text{Cr}_x\text{O}_2$  ( $x = 0, 0.05, 0.1, \text{ and } 0.2$ ) series. Apparently, the substitution of Ni/Mn with the redox active Cr, on the one hand, increases the amount of  $\text{Li}^+$  de-intercalated from the sloping region thanks to the contribution of the redox couple  $\text{Cr}^{3+/6+}$ , but at the same time decrease the LRLO structural stability due to the formation of  $\text{Cr}^{6+}$  centers and the distortion of the local coordination around the oxidized TM from octahedra to tetrahedra.

Sun et al. [117] investigated the effect of  $\text{Mg}^{2+}$  to replace the  $\text{Ni}^{2+}$  in  $\text{Li}[\text{Li}_{0.15}\text{Ni}_{0.275-x}\text{Mg}_x\text{Mn}_{0.575}]\text{O}_2$ . The Mg-doped LRLO showed an activated potentials profile

and after 50 cycles the specific capacities are 187, 185 and 183 mAhg<sup>-1</sup> respectively for x= 0, 0.02, and 0.04. Furthermore, the substitution of Ni<sup>2+</sup> with the smaller size Mg<sup>2+</sup> ions increase the structural stability without hindering the Li de-intercalation/intercalation from/into the lattice. Also, Wang et al. [118] focused on the evaluation of the effect of Mg doping on a Li<sub>1.2</sub>Ni<sub>0.2</sub>Mn<sub>0.6</sub>O<sub>2</sub> cathode and confirmed that the addition of a moderate amounts of Mg can stabilize the structure, keep high-capacity performance and increase ionic conductivity (e.g. the sample with 1% of Mg substitution of the Ni/Mn showed a discharge capacity of 226.5 mAhg<sup>-1</sup> after 60 cycles).

The effect of a simultaneous co-doping in a Co-free LRLO is less explored. Celeste et al. [15] investigated the substitution of Ni from Li<sub>1.2</sub>Mn<sub>0.6</sub>Ni<sub>0.2</sub>O<sub>2</sub> by the addition of Li- and Mn-, and optimized a material with formula Li<sub>1.25</sub>Ni<sub>0.125</sub>Mn<sub>0.625</sub>O<sub>2</sub>. The over-lithiation apparently suppress the first cycle high voltage plateau without major effects on the reversible capacity: during the first 50 cycles the optimized material showed an activated capacity trend and stabilized at 230 mAhg<sup>-1</sup> at C/10 (40 mA g<sup>-1</sup>).

Moving to anionic doping, Vanaphuti et al. [107] explored the effect of the incorporation of different anions (F<sup>-</sup>, S<sup>2-</sup> and Cl<sup>-</sup>) in the lattice of a Li<sub>1.2</sub>Mn<sub>0.6</sub>Ni<sub>0.2</sub>O<sub>2</sub> LRLO. They proved that, among all anionic dopants, F<sup>-</sup> increases the mean working potential, improves ionic conductivity, reduces cation mixing, and minimizes oxygen release. The LRLO phase doped with 1% of fluorine anions showed 95% of capacity retention after 100 cycles. Liu et al. [108] synthesized Li<sub>1.2</sub>Mn<sub>0.6</sub>Ni<sub>0.2</sub>O<sub>2</sub> doped with PO<sub>4</sub><sup>3-</sup> and co-doped Na<sup>+</sup>/PO<sub>4</sub><sup>3-</sup>. Double anion/cation doping promotes cycle stability with a capacity retention of 86.7% after 150 cycles and a good rate performance with 153 mAh g<sup>-1</sup> at 5C. The authors claimed that this strategy suppress the spinel transformation and improves the structural stability upon cycling. Also Nie et al. [119] used cation/anion co-doping of Li<sub>1.2</sub>Mn<sub>0.6</sub>Ni<sub>0.2</sub>O<sub>2</sub> with Fe and Cl and optimized the Li<sub>1.2</sub>Mn<sub>0.585</sub>Ni<sub>0.185</sub>Fe<sub>0.03</sub>O<sub>1.98</sub>Cl<sub>0.02</sub> composition. They demonstrated that a balanced co-doping promoted the lithium diffusion kinetic and reduced the oxygen redox reactivity, resulting in an improved Coulombic efficiency, better rate performance and long-term stability.

## 5. Conclusions

Li-rich layered oxides are one of the best alternative positive electrode active materials for the next-generation Li-ion batteries (i.e. generation 4a), thanks to the large specific capacity (>250 mAhg<sup>-1</sup>) and the highest specific energy (up to 900 WhKg<sup>-1</sup>) among all intercalation cathodes. LRLOs combines these excellent electrochemical properties with an improved environmental benignity thanks to the large content of manganese in their composition and the facile modification of the stoichiometry to reduce or remove cobalt. However, working potential fading, structural re-organization upon cycling, small Coulombic efficiency and unsatisfactory rate performance still hinder their transition from laboratory to manufacture and therefore the commercialization. As highlighted above, many of these drawbacks root in the complexity of their crystal structure and the elusive electrochemical reaction mechanism upon cycling in batteries. Large efforts are still spent worldwide to shed light on these fundamental features of LRLO: currently many discrepancies are still debated in literature and various hypothesis have been experimentally validated concerning both the crystal structure and the de-lithiation/lithiation mechanism. Apparently, the variability of the possible LRLO composition as well as the thermodynamic facility to incorporate defects in their structures make complex an unified model for the interpretation of both aspects.

The most relevant benefit of LRLO compared to stoichiometric layered phases (either Mn-rich, Ni-rich or balanced) is the possible complete removal of cobalt from their lattice without major impacts on the resulting electrochemical performance. This result can be obtained by a synergistic strategy that involves the optimization of the material preparation and a balanced cobalt substitution with other isovalent/aliovalent redox/non-redox cations. In fact, the use of different metal blends in the TM lattice, the optimization of the annealing temperatures, the incorporation of cationic or anionic dopants as well as the use

---

of coatings can alleviate the de-stabilization of the lattice induced by the  $\text{Co}^{3+}$  removal. Apparently, many different doping strategies have been proposed in the literature demonstrating various successful strategies to mitigate the working potential fading and to increase the structural resilience upon cycling LRLO. Also in this case, a generalized rationale is still missing, again likely due to the very wide variety of LRLO composition as well as the lack of a clear structural comprehension of these materials.

**Author Contributions:** All the authors contribute equally to the work. All authors have read and agreed to the published version of the manuscript.

**Funding:** L.S. received funds from Ministry of Ecological Transition in the framework of "Ricerca di Sistema Elettrico". The research project here reported was supported by the "Centro Nazionale per la Mobilità Sostenibile (MOST) CN4 Spoke 13 Batterie e Trazione Elettrica" funded by the Italian Government and the European Union in the frame of the "Missione 4 Componente 2 Investimento 1.4 -Potenziamento strutture di ricerca e creazione di "campioni nazionali di R&S" su alcune Key Enabling Technologies del PNRR (Avviso MUR n.3138 del 16-12-2021)".

**Data Availability Statement:** Not applicable

**Acknowledgments:** n/a

**Conflicts of Interest:** The authors declare no conflict of interest.

## References

1. Haas, J.; Cebulla, F.; Cao, K.; Nowak, W.; Palma-Behnke, R.; Rahmann, C.; Mancarella, P. Challenges and Trends of Energy Storage Expansion Planning for Flexibility Provision in Low-Carbon Power Systems – a Review. *Renewable and Sustainable Energy Reviews* **2017**, *80*, 603–619.
2. Winfield, M.; Shokrzadeh, S.; Jones, A. Energy Policy Regime Change and Advanced Energy Storage: A Comparative Analysis. *Energy Policy* **2018**, *115*, 572–583, doi:10.1016/j.enpol.2018.01.029.
3. Camargos, P.H.; dos Santos, P.H.J.; dos Santos, I.R.; Ribeiro, G.S.; Caetano, R.E. Perspectives on Li-Ion Battery Categories for Electric Vehicle Applications: A Review of State of the Art. *Int J Energy Res* **2022**, *46*, 19258–19268.
4. Zubi, G.; Dufo-López, R.; Carvalho, M.; Pasaoglu, G. The Lithium-Ion Battery: State of the Art and Future Perspectives. *Renewable and Sustainable Energy Reviews* **2018**, *89*, 292–308.
5. Grey, C.P.; Hall, D.S. Prospects for Lithium-Ion Batteries and beyond – a 2030 Vision. *Nat Commun* **2020**, *11*.
6. Finegan, D.P.; Squires, I.; Dahari, A.; Kench, S.; Jungjohann, K.L.; Cooper, S.J. Machine-Learning-Driven Advanced Characterization of Battery Electrodes. *ACS Energy Lett* **2022**, 4368–4378, doi:10.1021/acscenergylett.2c01996.
7. Bielewski, M.; Pfrang, A.; Bobba, S.; Kronberga, A.; Georgakaki, A.; Letout, S.; Grabowska, M. Clean Energy Technology Observatory, Batteries for Energy Storage in the European Union: Status Report on Technology Development, Trends, Value Chains and Markets: 2022, Publications Office of the European Union.; **2022**.
8. Tolganbek, N.; Yerkinbekova, Y.; Kalybekkyzy, S.; Bakenov, Z.; Mentbayeva, A. Current State of High Voltage Olivine Structured LiMPO<sub>4</sub> Cathode Materials for Energy Storage Applications: A Review. *J Alloys Compd* **2021**, 882.
9. Casas-Cabanas, M.; Ponrouch, A.; Palacín, M.R. Blended Positive Electrodes for Li-Ion Batteries: From Empiricism to Rational Design. *Isr J Chem* **2021**, *61*, 26–37.
10. Mohamed, N.; Allam, N.K. Recent Advances in the Design of Cathode Materials for Li-Ion Batteries. *RSC Adv* **2020**, *10*, 21662–21685.
11. Nie, L.; Chen, S.; Liu, W. Challenges and Strategies of Lithium-Rich Layered Oxides for Li-Ion Batteries. *Nano Res* **2022**.
12. Yang, J.; Niu, Y.; Wang, X.; Xu, M. A Review on the Electrochemical Reaction of Li-Rich Layered Oxide Materials. *Inorg Chem Front* **2021**, *8*, 4300–4312, doi:10.1039/D1QI00687H.
13. Li, W.; Song, B.; Manthiram, A. High-Voltage Positive Electrode Materials for Lithium-Ion Batteries. *Chem Soc Rev* **2017**, *46*, 3006–3059.
14. Jarvis, K.A.; Deng, Z.; Allard, L.F.; Manthiram, A.; Ferreira, P.J. Understanding Structural Defects in Lithium-Rich Layered Oxide Cathodes. *J Mater Chem* **2012**, *22*, 11550–11555, doi:10.1039/c2jm30575e.
15. Celeste, A.; Tuccillo, M.; Santoni, A.; Reale, P.; Brutti, S.; Silvestri, L. Exploring a Co-Free, Li-Rich Layered Oxide with Low Content of Nickel as a Positive Electrode for Li-Ion Battery. *ACS Appl Energy Mater* **2021**, *4*, 11290–11297, doi:10.1021/acsaem.1c02133.
16. Tuccillo, M.; Costantini, A.; Celeste, A.; García, A.B.M.; Pavone, M.; Paolone, A.; Palumbo, O.; Brutti, S. NAl/Li Antisite Defects in the Li<sub>1.2</sub>Ni<sub>0.2</sub>Mn<sub>0.6</sub>O<sub>2</sub> Li-Rich Layered Oxide: A DFT Study. *Crystals (Basel)* **2022**, *12*, doi:10.3390/cryst12050723.
17. Hwang, J.; Myeong, S.; Jin, W.; Jang, H.; Nam, G.; Yoon, M.; Kim, S.H.; Joo, S.H.; Kwak, S.K.; Kim, M.G.; et al. Excess-Li Localization Triggers Chemical Irreversibility in Li- and Mn-Rich Layered Oxides. *Advanced Materials* **2020**, *32*, doi:10.1002/adma.202001944.
18. Boulineau, A.; Croguennec, L.; Delmas, C.; Weill, F. Reinvestigation of Li<sub>2</sub>MnO<sub>3</sub> Structure: Electron Diffraction and High Resolution TEM. *Chemistry of Materials* **2009**, *21*, 4216–4222, doi:10.1021/cm900998n.
19. Hong, J.; Gwon, H.; Jung, S.-K.; Ku, K.; Kang, K. Review – Lithium-Excess Layered Cathodes for Lithium Rechargeable Batteries. *J Electrochem Soc* **2015**, *162*, A2447–A2467, doi:10.1149/2.0071514jes.
20. Thackeray, M.M.; Johnson, C.S.; Vaughey, J.T.; Li, N.; Hackney, S.A. Advances in Manganese-Oxide “composite” Electrodes for Lithium-Ion Batteries. *J Mater Chem* **2005**, *15*, 2257–2267, doi:10.1039/b417616m.
21. Wen, J.G.; Bareño, J.; Lei, C.H.; Kang, S.H.; Balasubramanian, M.; Petrov, I.; Abraham, D.P. Analytical Electron Microscopy of Li<sub>1.2</sub>Co<sub>0.4</sub>Mn<sub>0.4</sub>O<sub>2</sub> for Lithium-Ion Batteries. *Solid State Ion* **2011**, *182*, 98–107, doi:10.1016/j.ssi.2010.11.030.
22. Gu, M.; Genc, A.; Belharouak, I.; Wang, D.; Amine, K.; Thevuthasan, S.; Baer, D.R.; Zhang, J.G.; Browning, N.D.; Liu, J.; et al. Nanoscale Phase Separation, Cation Ordering, and Surface Chemistry in Pristine Li<sub>1.2</sub>Ni<sub>0.2</sub>Mn<sub>0.6</sub>O<sub>2</sub> for Li-Ion Batteries. *Chemistry of Materials* **2013**, *25*, 2319–2326, doi:10.1021/cm4009392.
23. Amalraj, F.; Kovacheva, D.; Talianker, M.; Zeiri, L.; Grinblat, J.; Leifer, N.; Goobes, G.; Markovsky, B.; Aurbach, D. Integrated Materials xLi<sub>2</sub>MnO<sub>3</sub>·(1-x)LiMn<sub>1/3</sub>Ni<sub>1/3</sub>Co<sub>1/3</sub>O<sub>2</sub> (X=0.3, 0.5, 0.7) Synthesized. *J Electrochem Soc* **2010**, *157*, A1121, doi:10.1149/1.3463782.
24. Nayak, P.K.; Yang, L.; Pollok, K.; Langenhorst, F.; Aurbach, D.; Adelhelm, P. Investigation of Li<sub>1.17</sub>Ni<sub>0.20</sub>Mn<sub>0.53</sub>Co<sub>0.10</sub>O<sub>2</sub> as an Interesting Li- and Mn-Rich Layered Oxide Cathode Material through Electrochemistry, Microscopy, and In Situ Electrochemical Dilatometry. *ChemElectroChem* **2019**, *6*, 2812–2819, doi:10.1002/celec.201900453.
25. Lu, Z.; Chen, Z.; Dahn, J.R. Lack of Cation Clustering in Li[Ni<sub>x</sub>Li<sub>1/3-2x/3</sub>Mn<sub>2/3-x/3</sub>]O<sub>2</sub> (0 < x ≤ 1/2) and Li[Cr<sub>x</sub>Li<sub>(1-x)/3</sub>Mn<sub>(2-2x)/3</sub>]O<sub>2</sub> (0 < x < 1). *Chemistry of Materials* **2003**, *15*, 3214–3220, doi:10.1021/cm030194s.

26. Koga, H.; Croguennec, L.; Mannesiez, P.; Ménétrier, M.; Weill, F.; Bourgeois, L.; Duttine, M.; Suard, E.; Delmas, C. Li<sub>1.20</sub>Mn<sub>0.54</sub>Co<sub>0.13</sub>Ni<sub>0.13</sub>O<sub>2</sub> with Different Particle Sizes as Attractive Positive Electrode Materials for Lithium-Ion Batteries: Insights into Their Structure. *Journal of Physical Chemistry C* **2012**, *116*, 13497–13506, doi:10.1021/jp301879x.
27. Jarvis, K.A.; Deng, Z.; Allard, L.F.; Manthiram, A.; Ferreira, P.J. Atomic Structure of a Lithium-Rich Layered Oxide Material for Lithium-Ion Batteries: Evidence of a Solid Solution. *Chemistry of Materials* **2011**, *23*, 3614–3621, doi:10.1021/cm200831c.
28. Ates, M.N.; Mukerjee, S.; Abraham, K.M. A High Rate Li-Rich Layered MNC Cathode Material for Lithium-Ion Batteries. *RSC Adv* **2015**, *5*, 27375–27386, doi:10.1039/c4ra17235c.
29. Boulineau, A.; Croguennec, L.; Delmas, C.; Weill, F. Structure of Li<sub>2</sub>MnO<sub>3</sub> with Different Degrees of Defects. *Solid State Ion* **2010**, *180*, 1652–1659, doi:10.1016/j.ssi.2009.10.020.
30. Seymour, I.D.; Middlemiss, D.S.; Halat, D.M.; Trease, N.M.; Pell, A.J.; Grey, C.P. Characterizing Oxygen Local Environments in Paramagnetic Battery Materials via <sup>17</sup>O NMR and DFT Calculations. *J Am Chem Soc* **2016**, *138*, 9405–9408, doi:10.1021/jacs.6b05747.
31. Lei, C.H.; Bareño, J.; Wen, J.G.; Petrov, I.; Kang, S.H.; Abraham, D.P. Local Structure and Composition Studies of Li<sub>1.2</sub>Ni<sub>0.2</sub>Mn<sub>0.6</sub>O<sub>2</sub> by Analytical Electron Microscopy. *J Power Sources* **2008**, *178*, 422–433, doi:10.1016/j.jpowsour.2007.11.077.
32. Jamil, S.; Li, C.; Fasihullah, M.; Liu, P.; Xiao, F.; Wang, H.; Bao, S.; Xu, M. Ni/Li Antisite Induced Disordered Passivation Layer for High-Ni Layered Oxide Cathode Material. *Energy Storage Mater* **2022**, *45*, 720–729, doi:10.1016/j.ensm.2021.12.025.
33. Tang, Z.; Wang, S.; Liao, J.; Wang, S.; He, X.; Pan, B.; He, H.; Chen, C. Facilitating Lithium-Ion Diffusion in Layered Cathode Materials by Introducing Li<sup>+</sup>/Ni<sup>2+</sup> Antisite Defects for High-Rate Li-Ion Batteries. *Research* **2019**, *2019*, 1–10, doi:10.34133/2019/2198906.
34. Serrano-Sevillano, J.; Reynaud, M.; Saracibar, A.; Altantzis, T.; Bals, S.; van Tendeloo, G.; Casas-Cabanas, M. Enhanced Electrochemical Performance of Li-Rich Cathode Materials through Microstructural Control. *Physical Chemistry Chemical Physics* **2018**, *20*, 23112–23122, doi:10.1039/c8cp04181d.
35. Matsunaga, T.; Komatsu, H.; Shimoda, K.; Minato, T.; Yonemura, M.; Kamiyama, T.; Kobayashi, S.; Kato, T.; Hirayama, T.; Ikuhara, Y.; et al. Dependence of Structural Defects in Li<sub>2</sub>MnO<sub>3</sub> on Synthesis Temperature. *Chemistry of Materials* **2016**, *28*, 4143–4150, doi:10.1021/acs.chemmater.5b05041.
36. Menon, A.S.; Khalil, S.; Ojwang, D.O.; Edström, K.; Gomez, C.P.; Brant, W.R. Synthesis-Structure Relationships in Li- and Mn-Rich Layered Oxides: Phase Evolution, Superstructure Ordering and Stacking Faults. *Dalton Transactions* **2022**, *51*, 4435–4446, doi:10.1039/d2dt00104g.
37. Menon, A.S.; Ulusoy, S.; Ojwang, D.O.; Riekehr, L.; Didier, C.; Peterson, V.K.; Salazar-Alvarez, G.; Svedlindh, P.; Edstrom, K.; Gomez, C.P.; et al. Synthetic Pathway Determines the Nonequilibrium Crystallography of Li- and Mn-Rich Layered Oxide Cathode Materials. *ACS Appl Energy Mater* **2021**, *4*, 1924–1935, doi:10.1021/acsaem.0c03027.
38. Ma, D.; Li, Y.; Zhang, P.; Cooper, A.J.; Abdelkader, A.M.; Ren, X.; Deng, L. Mesoporous Li<sub>1.2</sub>Mn<sub>0.54</sub>Ni<sub>0.13</sub>Co<sub>0.13</sub>O<sub>2</sub> Nanotubes for High-Performance Cathodes in Li-Ion Batteries. *J Power Sources* **2016**, *311*, 35–41, doi:10.1016/j.jpowsour.2016.01.031.
39. Wang, J.; He, X.; Paillard, E.; Laszczynski, N.; Li, J.; Passerini, S. Lithium- and Manganese-Rich Oxide Cathode Materials for High-Energy Lithium Ion Batteries. *Adv Energy Mater* **2016**, *6*, 1600906, doi:10.1002/aenm.201600906.
40. Buchholz, D.; Li, J.; Passerini, S.; Aquilanti, G.; Wang, D.; Giorgetti, M. X-Ray Absorption Spectroscopy Investigation of Lithium-Rich, Cobalt-Poor Layered-Oxide Cathode Material with High Capacity. *ChemElectroChem* **2015**, *2*, 85–97, doi:10.1002/celec.201402324.
41. Zhao, S.; Yan, K.; Zhang, J.; Sun, B.; Wang, G. Reaction Mechanisms of Layered Lithium-Rich Cathode Materials for High-Energy Lithium-Ion Batteries. *Angewandte Chemie - International Edition* **2021**, *60*, 2208–2220.
42. Lu, Z.; Dahn, J.R. Understanding the Anomalous Capacity of Li/Li[Ni<sub>x</sub>Li<sub>(1/3-2x/3)</sub>Mn<sub>(2/3-x/3)</sub>]O<sub>2</sub> Cells Using In Situ X-Ray Diffraction and Electrochemical Studies. *J Electrochem Soc* **2002**, *149*, A815, doi:10.1149/1.1480014.
43. Ji, X.; Xia, Q.; Xu, Y.; Feng, H.; Wang, P.; Tan, Q. A Review on Progress of Lithium-Rich Manganese-Based Cathodes for Lithium Ion Batteries. *J Power Sources* **2021**, *487*, 229362, doi:10.1016/j.jpowsour.2020.229362.
44. Pan, H.; Zhang, S.; Chen, J.; Gao, M.; Liu, Y.; Zhu, T.; Jiang, Y. Li- and Mn-Rich Layered Oxide Cathode Materials for Lithium-Ion Batteries: A Review from Fundamentals to Research Progress and Applications. *Mol Syst Des Eng* **2018**, *3*, 748–803.
45. Strehle, B.; Kleiner, K.; Jung, R.; Chesneau, F.; Mendez, M.; Gasteiger, H.A.; Piana, M. The Role of Oxygen Release from Li- and Mn-Rich Layered Oxides during the First Cycles Investigated by On-Line Electrochemical Mass Spectrometry. *J Electrochem Soc* **2017**, *164*, A400–A406, doi:10.1149/2.1001702jes.
46. Armstrong, A.R.; Holzappel, M.; Nová, P.; Johnson, C.S.; Kang, S.-H.; Thackeray, M.M.; Bruce, P.G. Demonstrating Oxygen Loss and Associated Structural Reorganization in the Lithium Battery Cathode Li[Ni<sub>0.2</sub>Li<sub>0.2</sub>Mn<sub>0.6</sub>]O<sub>2</sub>. *J Am Chem Soc* **2006**, *128*, 8694–8698, doi:10.1021/ja062027.

47. Sathiya, M.; Rouse, G.; Ramesha, K.; Laisa, C.P.; Vezin, H.; Sougrati, M.T.; Doublet, M.L.; Foix, D.; Gonbeau, D.; Walker, W.; et al. Reversible Anionic Redox Chemistry in High-Capacity Layered-Oxide Electrodes. *Nat Mater* **2013**, *12*, 827–835, doi:10.1038/nmat3699.
48. Sathiya, M.; Ramesha, K.; Rouse, G.; Foix, D.; Gonbeau, D.; Prakash, A.S.; Doublet, M.L.; Hemalatha, K.; Tarascon, J.M. High Performance  $\text{Li}_2\text{Ru}_{1-y}\text{Mn}_y\text{O}_3$  ( $0.2 \leq y \leq 0.8$ ) Cathode Materials for Rechargeable Lithium-Ion Batteries: Their Understanding. *Chemistry of Materials* **2013**, *25*, 1121–1131, doi:10.1021/cm400193m.
49. Li, X.; Qiao, Y.; Guo, S.; Xu, Z.; Zhu, H.; Zhang, X.; Yuan, Y.; He, P.; Ishida, M.; Zhou, H. Direct Visualization of the Reversible  $\text{O}^{2-}/\text{O}^-$  Redox Process in Li-Rich Cathode Materials. *Advanced Materials* **2018**, *30*, 1705197, doi:10.1002/adma.201705197.
50. Chen, H.; Islam, M.S. Lithium Extraction Mechanism in Li-Rich  $\text{Li}_2\text{MnO}_3$  Involving Oxygen Hole Formation and Dimerization. *Chemistry of Materials* **2016**, *28*, 6656–6663, doi:10.1021/acs.chemmater.6b02870.
51. Luo, K.; Roberts, M.R.; Guerrini, N.; Tapia-Ruiz, N.; Hao, R.; Massel, F.; Pickup, D.M.; Ramos, S.; Liu, Y.S.; Guo, J.; et al. Anion Redox Chemistry in the Cobalt Free 3d Transition Metal Oxide Intercalation Electrode  $\text{Li}[\text{Li}_{0.2}\text{Ni}_{0.2}\text{Mn}_{0.6}]\text{O}_2$ . *J Am Chem Soc* **2016**, *138*, 11211–11218, doi:10.1021/jacs.6b05111.
52. Luo, K.; Roberts, M.R.; Hao, R.; Guerrini, N.; Pickup, D.M.; Liu, Y.S.; Edström, K.; Guo, J.; Chadwick, A. v.; Duda, L.C.; et al. Charge-Compensation in 3d-Transition-Metal-Oxide Intercalation Cathodes through the Generation of Localized Electron Holes on Oxygen. *Nat Chem* **2016**, *8*, 684–691, doi:10.1038/nchem.2471.
53. Gent, W.E.; Lim, K.; Liang, Y.; Li, Q.; Barnes, T.; Ahn, S.J.; Stone, K.H.; McIntire, M.; Hong, J.; Song, J.H.; et al. Coupling between Oxygen Redox and Cation Migration Explains Unusual Electrochemistry in Lithium-Rich Layered Oxides. *Nat Commun* **2017**, *8*, 1–12, doi:10.1038/s41467-017-02041-x.
54. Fell, C.R.; Qian, D.; Carroll, K.J.; Chi, M.; Jones, J.L.; Meng, Y.S. Correlation between Oxygen Vacancy, Microstrain, and Cation Distribution in Lithium-Excess Layered Oxides during the First Electrochemical Cycle. *Chemistry of Materials* **2013**, *25*, 1621–1629, doi:10.1021/cm4000119.
55. Zuo, W.; Luo, M.; Liu, X.; Wu, J.; Liu, H.; Li, J.; Winter, M.; Fu, R.; Yang, W.; Yang, Y. Li-Rich Cathodes for Rechargeable Li-Based Batteries: Reaction Mechanisms and Advanced Characterization Techniques. *Energy Environ Sci* **2020**, *13*, 4450–4497.
56. Assat, G.; Foix, D.; Delacourt, C.; Iadecola, A.; Dedryvère, R.; Tarascon, J.M. Fundamental Interplay between Anionic/Cationic Redox Governing the Kinetics and Thermodynamics of Lithium-Rich Cathodes. *Nat Commun* **2017**, *8*, doi:10.1038/s41467-017-02291-9.
57. Tao, S.; Huang, W.; Chu, S.; Qian, B.; Liu, L.; Xu, W. Dynamic Structural Evolution of Oxygen Vacancies in Lithium Rich Layered Composites Cathodes for Li-Ion Batteries. *Materials Today Physics* **2021**, *18*, doi:10.1016/j.mtphys.2021.100403.
58. Cui, S.L.; Wang, Y.Y.; Liu, S.; Li, G.R.; Gao, X.P. Evolution Mechanism of Phase Transformation of Li-Rich Cathode Materials in Cycling. *Electrochim Acta* **2019**, *328*, doi:10.1016/j.electacta.2019.135109.
59. Xu, B.; Fell, C.R.; Chi, M.; Meng, Y.S. Identifying Surface Structural Changes in Layered Li-Excess Nickel Manganese Oxides in High Voltage Lithium Ion Batteries: A Joint Experimental and Theoretical Study. *Energy Environ Sci* **2011**, *4*, 2223–2233, doi:10.1039/c1ee01131f.
60. Boulineau, A.; Simonin, L.; Colin, J.F.; Bourbon, C.; Patoux, S. First Evidence of Manganese-Nickel Segregation and Densification upon Cycling in Li-Rich Layered Oxides for Lithium Batteries. *Nano Lett* **2013**, *13*, 3857–3863, doi:10.1021/nl4019275.
61. Koga, H.; Croguennec, L.; Ménétrier, M.; Douhil, K.; Belin, S.; Bourgeois, L.; Suard, E.; Weill, F.; Delmas, C. Reversible Oxygen Participation to the Redox Processes Revealed for  $\text{Li}_{1.20}\text{Mn}_{0.54}\text{Co}_{0.13}\text{Ni}_{0.13}\text{O}_2$ . *J Electrochem Soc* **2013**, *160*, A786–A792, doi:10.1149/2.038306jes.
62. Koga, H.; Croguennec, L.; Ménétrier, M.; Mannesiez, P.; Weill, F.; Delmas, C. Different Oxygen Redox Participation for Bulk and Surface: A Possible Global Explanation for the Cycling Mechanism of  $\text{Li}_{1.20}\text{Mn}_{0.54}\text{Co}_{0.13}\text{Ni}_{0.13}\text{O}_2$ . *J Power Sources* **2013**, *236*, 250–258, doi:10.1016/j.jpowsour.2013.02.075.
63. Celeste, A.; Girardi, F.; Gigli, L.; Pellegrini, V.; Silvestri, L.; Brutti, S. Impact of Overlithiation and Al Doping on the Battery Performance of Li-Rich Layered Oxide Materials. *Electrochim Acta* **2022**, *428*, 140737, doi:10.1016/j.electacta.2022.140737.
64. Celeste, A.; Brescia, R.; Gigli, L.; Plaisier, J.; Pellegrini, V.; Silvestri, L.; Brutti, S. Unravelling Structural Changes of the  $\text{Li}_{1.2}\text{Mn}_{0.54}\text{Ni}_{0.13}\text{Co}_{0.13}\text{O}_2$  Lattice upon Cycling in Lithium Cell. *Materials Today Sustainability* **2022**, 100277, doi:10.1016/j.mtsust.2022.100277.
65. Robertson, A.D.; Bruce, P.G. Overcapacity of  $\text{Li}[\text{Ni}_x\text{Li}_{1/3-2x/3}\text{Mn}_{2/3-x/3}]\text{O}_2$  Electrodes. *Electrochemical and Solid-State Letters* **2004**, *7*, doi:10.1149/1.1783114.
66. Tran, N.; Croguennec, L.; Ménétrier, M.; Weill, F.; Biensan, P.; Jordy, C.; Delmas, C. Mechanisms Associated with the “Plateau” Observed at High Voltage for the Overlithiated  $\text{Li}_{1.12}(\text{Ni}_{0.425}\text{Mn}_{0.425}\text{Co}_{0.15})_{0.88}\text{O}_2$  System. *Chemistry of Materials* **2008**, *20*, 4815–4825, doi:10.1021/cm070435m.
67. Lu, Z.; MacNeil, D.D.; Dahn, J.R. Layered Cathode Materials  $\text{Li}[\text{Ni}_x\text{Li}_{(1/3-2x/3)}\text{Mn}_{(2/3-x/3)}]\text{O}_2$  for Lithium-Ion Batteries. *Electrochemical and Solid-State Letters* **2001**, *4*, doi:10.1149/1.1407994.

68. Oishi, M.; Yogi, C.; Watanabe, I.; Ohta, T.; Orikasa, Y.; Uchimoto, Y.; Ogumi, Z. Direct Observation of Reversible Charge Compensation by Oxygen Ion in Li-Rich Manganese Layered Oxide Positive Electrode Material,  $\text{Li}_{1.16}\text{Ni}_{0.15}\text{Co}_{0.19}\text{Mn}_{0.50}\text{O}_2$ . *J Power Sources* **2015**, *276*, 89–94, doi:10.1016/j.jpowsour.2014.11.104.
69. Kang, S.H.; Sun, Y.K.; Amine, K. Electrochemical and Ex Situ X-Ray Study of  $\text{Li}(\text{Li}_{0.2}\text{Ni}_{0.2}\text{Mn}_{0.6})\text{O}_2$  Cathode Material for Li Secondary Batteries. *Electrochemical and Solid-State Letters* **2003**, *6*, doi:10.1149/1.1594411.
70. Seo, D.H.; Lee, J.; Urban, A.; Malik, R.; Kang, S.; Ceder, G. The Structural and Chemical Origin of the Oxygen Redox Activity in Layered and Cation-Disordered Li-Excess Cathode Materials. *Nat Chem* **2016**, *8*, 692–697, doi:10.1038/nchem.2524.
71. Armstrong, A.R.; Robertson, A.D.; Bruce, P.G. Overcharging Manganese Oxides: Extracting Lithium beyond  $\text{Mn}^{4+}$ . In Proceedings of the Journal of Power Sources; August 26 2005; Vol. 146, pp. 275–280. doi: 10.1016/j.jpowsour.2005.03.104
72. La Mantia, F.; Rosciano, F.; Tran, N.; Novák, P. Direct Evidence of Oxygen Evolution from  $\text{Li}_{1+x}(\text{Ni}_{1/3}\text{Mn}_{1/3}\text{Co}_{1/3})_{1-x}\text{O}_2$  at High Potentials. *J Appl Electrochem* **2008**, *38*, 893–896, doi:10.1007/s10800-008-9491-9.
73. Gao, Y.; Wang, X.; Ma, J.; Wang, Z.; Chen, L. Selecting Substituent Elements for Li-Rich Mn-Based Cathode Materials by Density Functional Theory (DFT) Calculations. *Chemistry of Materials* **2015**, *27*, 3456–3461, doi:10.1021/acs.chemmater.5b00875.
74. Hu, E.; Yu, X.; Lin, R.; Bi, X.; Lu, J.; Bak, S.; Nam, K.W.; Xin, H.L.; Jaye, C.; Fischer, D.A.; et al. Evolution of Redox Couples in Li- and Mn-Rich Cathode Materials and Mitigation of Voltage Fade by Reducing Oxygen Release. *Nat Energy* **2018**, *3*, 690–698, doi:10.1038/s41560-018-0207-z.
75. Gu, M.; Belharouak, I.; Zheng, J.; Wu, H.; Xiao, J.; Genc, A.; Amine, K.; Thevuthasan, S.; Baer, D.R.; Zhang, J.G.; et al. Formation of the Spinel Phase in the Layered Composite Cathode Used in Li-Ion Batteries. *ACS Nano* **2013**, *7*, 760–767, doi:10.1021/nn305065u.
76. Hong, J.; Seo, D.H.; Kim, S.W.; Gwon, H.; Oh, S.T.; Kang, K. Structural Evolution of Layered  $\text{Li}_{1.2}\text{Ni}_{0.2}\text{Mn}_{0.6}\text{O}_2$  upon Electrochemical Cycling in a Li Rechargeable Battery. *J Mater Chem* **2010**, *20*, 10179–10186, doi:10.1039/c0jm01971b.
77. Yin, W.; Grimaud, A.; Rousse, G.; Abakumov, A.M.; Senyshyn, A.; Zhang, L.; Trabesinger, S.; Iadecola, A.; Foix, D.; Giaume, D.; et al. Structural Evolution at the Oxidative and Reductive Limits in the First Electrochemical Cycle of  $\text{Li}_{1.2}\text{Ni}_{0.13}\text{Mn}_{0.54}\text{Co}_{0.13}\text{O}_2$ . *Nat Commun* **2020**, *11*, doi:10.1038/s41467-020-14927-4.
78. COMMITTEE OF THE REGIONS AND THE EUROPEAN INVESTMENT BANK on the Implementation of the Strategic Action Plan on Batteries: Building a Strategic Battery Value Chain in Europe;
79. GROW - Internal Market, D.D. 245 Final COMMISSION STAFF WORKING DOCUMENT Report on Raw Materials for Battery Applications;
80. Kugel', K.I.; Khomskii, D.I. *Lebedev Physics Institute, Academy of Sciences of the USSR, Moscow and Institute of High Temperatures*; **1982**; Vol. 136;.
81. Tuccillo, M.; Mei, L.; Palumbo, O.; Muñoz-García, A.B.; Pavone, M.; Paolone, A.; Brutti, S. Replacement of Cobalt in Lithium-Rich Layered Oxides by n-Doping: A Dft Study. *Applied Sciences (Switzerland)* **2021**, *11*, doi:10.3390/app112210545.
82. Kou, J.; Chen, L.; Su, Y.; Bao, L.; Wang, J.; Li, N.; Li, W.; Wang, M.; Chen, S.; Wu, F. Role of Cobalt Content in Improving the Low-Temperature Performance of Layered Lithium-Rich Cathode Materials for Lithium-Ion Batteries. *ACS Appl Mater Interfaces* **2015**, *7*, 17910–17918, doi:10.1021/acsami.5b04514.
83. Ramesha, R.N.; Bosubabu, D.; Karthick Babu, M.G.; Ramesha, K. Tuning of Ni, Mn, and Co (NMC) Content in  $0.4(\text{LiNi}_x\text{Mn}_y\text{Co}_z\text{O}_2)\cdot 0.4(\text{Li}_2\text{MnO}_3)$  toward Stable High-Capacity Lithium-Rich Cathode Materials. *ACS Appl Energy Mater* **2020**, *3*, 10872–10881, doi:10.1021/acsaem.0c01897.
84. Redel, K.; Kulka, A.; Plewa, A.; Molenda, J. High-Performance Li-Rich Layered Transition Metal Oxide Cathode Materials for Li-Ion Batteries. *J Electrochem Soc* **2019**, *166*, A5333–A5342, doi:10.1149/2.0511903jes.
85. Hamad, K.I.; Xing, Y. Effect of Cobalt and Nickel Contents on the Performance of Lithium Rich Materials Synthesized in Glycerol Solvent. *J Electrochem Soc* **2018**, *165*, A2470–A2475, doi:10.1149/2.0311811jes.
86. Bao, L.; Yang, Z.; Chen, L.; Su, Y.; Lu, Y.; Li, W.; Yuan, F.; Dong, J.; Fang, Y.; Ji, Z.; et al. The Effects of Trace Yb Doping on the Electrochemical Performance of Li-Rich Layered Oxides. *ChemSusChem* **2019**, *12*, 2294–2301, doi:10.1002/cssc.201900226.
87. Kou, Y.; Han, E.; Zhu, L.Z.; Liu, L.; Zhang, Z. The Effect of Ti Doping on Electrochemical Properties of  $\text{Li}_{1.167}\text{Ni}_{0.4}\text{Mn}_{0.383}\text{Co}_{0.05}\text{O}_2$  for Lithium-Ion Batteries. *Solid State Ion* **2016**, *296*, 154–157, doi:10.1016/j.ssi.2016.09.020.
88. Guo, H.; Xia, Y.; Zhao, H.; Yin, C.; Jia, K.; Zhao, F.; Liu, Z. Stabilization Effects of Al Doping for Enhanced Cycling Performances of Li-Rich Layered Oxides. *Ceram Int* **2017**, *43*, 13845–13852, doi:10.1016/j.ceramint.2017.07.107.
89. Tang, T.; Zhang, H.L. Synthesis and Electrochemical Performance of Lithium-Rich Cathode Material  $\text{Li}[\text{Li}_{0.2}\text{Ni}_{0.15}\text{Mn}_{0.55}\text{Co}_{0.1-x}\text{Al}_x]\text{O}_2$ . *Electrochim Acta* **2016**, *191*, 263–269, doi:10.1016/j.electacta.2016.01.066.
90. Dong, S.; Zhou, Y.; Hai, C.; Zeng, J.; Sun, Y.; Shen, Y.; Li, X.; Ren, X.; Sun, C.; Zhang, G.; et al. Understanding Electrochemical Performance Improvement with Nb Doping in Lithium-Rich Manganese-Based Cathode Materials. *J Power Sources* **2020**, *462*, doi:10.1016/j.jpowsour.2020.228185.

91. Liu, X.; Yu, B.; Wang, M.; Jin, Y.; Fu, Z.; Chen, J.; Ma, Z.; Guo, B.; Huang, Y.; Li, X. Electrochemical Performances of Niobium-Doped New Spherical Low-Cobalt Li-Rich Mn-Based  $\text{Li}_{1.14}\text{Mn}_{0.476}\text{Ni}_{0.254}\text{Co}_{0.048}\text{Al}_{0.016}\text{O}_2$  Cathode. *Mater Today Commun* **2022**, *32*, doi:10.1016/j.mtcomm.2022.104170.
92. Nayak, P.K.; Grinblat, J.; Levi, M.; Haik, O.; Levi, E.; Aurbach, D. Effect of Fe in Suppressing the Discharge Voltage Decay of High Capacity Li-Rich Cathodes for Li-Ion Batteries. *Journal of Solid State Electrochemistry* **2015**, *19*, 2781–2792, doi:10.1007/s10008-015-2790-2.
93. Yi, T.F.; Li, Y.M.; Cai, X.D.; Yang, S.Y.; Zhu, Y.R. Fe-Stabilized Li-Rich Layered  $\text{Li}_{1.2}\text{Mn}_{0.56}\text{Ni}_{0.16}\text{Co}_{0.08}\text{O}_2$  Oxide as a High Performance Cathode for Advanced Lithium-Ion Batteries. *Mater Today Energy* **2017**, *4*, 25–33, doi:10.1016/j.mtener.2017.03.005.
94. Medvedeva, A.; Makhonina, E.; Pechen, L.; Politov, Y.; Rumyantsev, A.; Koshtyal, Y.; Goloveshkin, A.; Maslakov, K.; Eremenko, I. Effect of Al and Fe Doping on the Electrochemical Behavior of  $\text{Li}_{1.2}\text{Ni}_{0.133}\text{Mn}_{0.534}\text{Co}_{0.133}\text{O}_2$  Li-Rich Cathode Material. *Materials* **2022**, *15*, doi:10.3390/ma15228225.
95. Nisar, U.; Amin, R.; Shakoor, A.; Essehli, R.; Al-Qaradawi, S.; Kahraman, R.; Belharouak, I. Synthesis and Electrochemical Characterization of Cr-Doped Lithium-Rich  $\text{Li}_{1.2}\text{Ni}_{0.16}\text{Mn}_{0.56}\text{Co}_{0.08-x}\text{Cr}_x\text{O}_2$  Cathodes. *Emergent Mater* **2018**, *1*, 155–164, doi:10.1007/s42247-018-0014-0.
96. Ghorbanzadeh, M.; Allahyari, E.; Riahifar, R.; Hadavi, S.M.M. Effect of Al and Zr Co-Doping on Electrochemical Performance of Cathode  $\text{Li}[\text{Li}_{0.2}\text{Ni}_{0.13}\text{Co}_{0.13}\text{Mn}_{0.54}]\text{O}_2$  for Li-Ion Battery. *Journal of Solid State Electrochemistry* **2018**, *22*, 1155–1163, doi:10.1007/s10008-017-3824-8.
97. Celeste, A.; Brescia, R.; Greco, G.; Torelli, P.; Mauri, S.; Silvestri, L.; Pellegrini, V.; Brutti, S. Pushing Stoichiometries of Lithium-Rich Layered Oxides Beyond Their Limits. *ACS Appl Energy Mater* **2022**, acaem.1c03396, doi:10.1021/acsaem.1c03396.
98. Feng, Z.; Song, H.; Li, Y.; Lyu, Y.; Xiao, D.; Guo, B. Adjusting Oxygen Redox Reaction and Structural Stability of Li- and Mn-Rich Cathodes by Zr-Ti Dual-Doping. *ACS Appl Mater Interfaces* **2022**, *14*, 5308–5317, doi:10.1021/acsaem.1c20880.
99. Zhang, H.Z.; Qiao, Q.Q.; Li, G.R.; Gao, X.P.  $\text{PO}_4^{3-}$  Polyanion-Doping for Stabilizing Li-Rich Layered Oxides as Cathode Materials for Advanced Lithium-Ion Batteries. *J Mater Chem A Mater* **2014**, *2*, 7454–7460, doi:10.1039/c4ta00699b.
100. Zhang, H.-Z.; Li, F.; Pan, G.-L.; Li, G.-R.; Gao, X.-P. The Effect of Polyanion-Doping on the Structure and Electrochemical Performance of Li-Rich Layered Oxides as Cathode for Lithium-Ion Batteries. *J Electrochem Soc* **2015**, *162*, A1899–A1904, doi:10.1149/2.1031509jes.
101. Thackeray, M.M.; Kang, S.H.; Johnson, C.S.; Vaughey, J.T.; Hackney, S.A. Comments on the Structural Complexity of Lithium-Rich  $\text{Li}_{1-x}\text{M}_{1-x}\text{O}_2$  Electrodes (M = Mn, Ni, Co) for Lithium Batteries. *Electrochem Commun* **2006**, *8*, 1531–1538, doi:10.1016/j.elecom.2006.06.030.
102. Wang, C.C.; Jarvis, K.A.; Ferreira, P.J.; Manthiram, A. Effect of Synthesis Conditions on the First Charge and Reversible Capacities of Lithium-Rich Layered Oxide Cathodes. *Chemistry of Materials* **2013**, *25*, 3267–3275, doi:10.1021/cm402181f.
103. Rajappa Prakasha, K.; Grins, J.; Jaworski, A.; Thersleff, T.; Svensson, G.; Jøsang, L.O.; Dyrli, A.D.; Paulus, A.; de Sloovere, D.; D’Haen, J.; et al. Temperature-Driven Chemical Segregation in Co-Free Li-Rich-Layered Oxides and Its Influence on Electrochemical Performance. *Chemistry of Materials* **2022**, *34*, 3637–3647, doi:10.1021/acs.chemmater.1c04150.
104. Jiang, W.; Zhang, C.; Feng, Y.; Wei, B.; Chen, L.; Zhang, R.; Ivey, D.G.; Wang, P.; Wei, W. Achieving High Structure and Voltage Stability in Cobalt-Free Li-Rich Layered Oxide Cathodes via Selective Dual-Cation Doping. *Energy Storage Mater* **2020**, *32*, 37–45, doi:10.1016/j.ensm.2020.07.035.
105. Zheng, H.; Zhang, C.; Zhang, Y.; Lin, L.; Liu, P.; Wang, L.; Wei, Q.; Lin, J.; Sa, B.; Xie, Q.; et al. Manipulating the Local Electronic Structure in Li-Rich Layered Cathode Towards Superior Electrochemical Performance. *Adv Funct Mater* **2021**, *31*, doi:10.1002/adfm.202100783.
106. Yu, Y.; Yang, Z.; Zhong, J.; Liu, Y.; Li, J.; Wang, X.; Kang, F. A Simple Dual-Ion Doping Method for Stabilizing Li-Rich Materials and Suppressing Voltage Decay. *ACS Appl Mater Interfaces* **2020**, *12*, 13996–14004, doi:10.1021/acsaem.0c00944.
107. Vanaphuti, P.; Bong, S.; Ma, L.; Ehrlich, S.; Wang, Y. Systematic Study of Different Anion Doping on the Electrochemical Performance of Cobalt-Free Lithium-Manganese-Rich Layered Cathode. *ACS Appl Energy Mater* **2020**, *3*, 4852–4859, doi:10.1021/acsaem.0c00439.
108. Liu, H.; He, B.; Xiang, W.; Li, Y.C.; Bai, C.; Liu, Y.P.; Zhou, W.; Chen, X.; Liu, Y.; Gao, S.; et al. Synergistic Effect of Uniform Lattice Cation/Anion Doping to Improve Structural and Electrochemical Performance Stability for Li-Rich Cathode Materials. *Nanotechnology* **2020**, *31*, doi:10.1088/1361-6528/ab9579.
109. Wang, C.C.; Manthiram, A. Influence of Cationic Substitutions on the First Charge and Reversible Capacities of Lithium-Rich Layered Oxide Cathodes. *J Mater Chem A Mater* **2013**, *1*, 10209–10217, doi:10.1039/C3TA11703K.
110. Deng, Z.Q.; Manthiram, A. Influence of Cationic Substitutions on the Oxygen Loss and Reversible Capacity of Lithium-Rich Layered Oxide Cathodes. *Journal of Physical Chemistry C* **2011**, *115*, 7097–7103, doi: 10.1021/jp200375d
111. Laisa, C.P.; Nanda Kumar, A.K.; Selva Chandrasekaran, S.; Murugan, P.; Lakshminarasimhan, N.; Govindaraj, R.; Ramesha, K. A Comparative Study on Electrochemical Cycling Stability of Lithium Rich Layered Cathode Materials  $\text{Li}_{1.2}\text{Ni}_{0.13}\text{M}_{0.13}\text{Mn}_{0.54}\text{O}_2$  Where M = Fe or Co. *J Power Sources* **2016**, *324*, 462–474, doi:10.1016/J.JPOWSOUR.2016.05.107.

112. Wu, F.; Kim, G.T.; Kuenzel, M.; Zhang, H.; Asenbauer, J.; Geiger, D.; Kaiser, U.; Passerini, S. Elucidating the Effect of Iron Doping on the Electrochemical Performance of Cobalt-Free Lithium-Rich Layered Cathode Materials. *Adv Energy Mater* **2019**, *9*, doi:10.1002/aenm.201902445.
113. Wei, H.; Cheng, X.; Fan, H.; Shan, Q.; An, S.; Qiu, X.; Jia, G. A Cobalt-Free  $\text{Li}(\text{Li}_{0.17}\text{Ni}_{0.17}\text{Fe}_{0.17}\text{Mn}_{0.49})\text{O}_2$  Cathode with More Oxygen-Involving Charge Compensation for Lithium-Ion Batteries. *ChemSusChem* **2019**, *12*, 2471–2479, doi:10.1002/cssc.201900241.
114. Pham, H.Q.; Kondracki, Ł.; Tarik, M.; Trabesinger, S. Correlating the Initial Gas Evolution and Structural Changes to Cycling Performance of Co-Free Li-Rich Layered Oxide Cathode. *J Power Sources* **2022**, *527*, doi:10.1016/j.jpowsour.2022.231181.
115. Lu, Z.; Dahn, J.R. Structure and Electrochemistry of Layered  $\text{Li}[\text{Cr}_{(1/3-x/3)}\text{Mn}_{(2/3-2x/3)}]\text{O}_2$ . *J Electrochem Soc* **2002**, *149*, A1454, doi:10.1149/1.1513557.
116. Lee, E.; Park, J.S.; Wu, T.; Sun, C.J.; Kim, H.; Stair, P.C.; Lu, J.; Zhou, D.; Johnson, C.S. Role of  $\text{Cr}^{3+}/\text{Cr}^{6+}$  Redox in Chromium-Substituted  $\text{Li}_2\text{MnO}_3 \cdot \text{LiNi}_{1/2}\text{Mn}_{1/2}\text{O}_2$  Layered Composite Cathodes: Electrochemistry and Voltage Fade. *J Mater Chem A Mater* **2015**, *3*, 9915–9924, doi:10.1039/C5TA01214G.
117. Sun, Y.K.; Kim, M.G.; Kang, S.H.; Amine, K. Electrochemical Performance of Layered  $\text{Li}[\text{Li}_{0.15}\text{Ni}_{0.275-x}\text{Mg}_x\text{Mn}_{0.575}]\text{O}_2$  Cathode Materials for Lithium Secondary Batteries. *J Mater Chem* **2003**, *13*, 319–322, doi:10.1039/B209379K.
118. Wang, D.; Huang, Y.; Huo, Z.; Chen, L. Synthesize and Electrochemical Characterization of Mg-Doped Li-Rich Layered  $\text{Li}[\text{Li}_{0.2}\text{Ni}_{0.2}\text{Mn}_{0.6}]\text{O}_2$  Cathode Material. *Electrochim Acta* **2013**, *107*, 461–466, doi:10.1016/J.ELECTACTA.2013.05.145.
119. Nie, L.; Wang, Z.; Zhao, X.; Chen, S.; He, Y.; Zhao, H.; Gao, T.; Zhang, Y.; Dong, L.; Kim, F.; et al. Cation/Anion Codoped and Cobalt-Free Li-Rich Layered Cathode for High-Performance Li-Ion Batteries. *Nano Lett* **2021**, *21*, 8370–8377, doi:10.1021/acs.nanolett.1c02923.